Spring 5-31-1984

Behavior of thin-walled channel shaped reinforced concrete columns under combined biaxial bending and compression

Subash Yalamarthy
New Jersey Institute of Technology

BEHAVIOR OF THIN-WALLED CHANNEL SHAPED REINFORCED CONCRETE COLUMNS UNDER COMBINED BIAXIAL BENDING AND COMPRESSION

by

SUBASH YALAMARTHY

Thesis submitted to the Faculty of the Graduate School of the New Jersey Institute of Technology in partial fulfillment of the requirements for the degree of Master of Science in Civil Engineering
1984

APPROVAL SHEET

Title of Thesis: Behavior of Thin-Walled Channel Shaped Reinforced Concrete Columns under combined Biaxial Bending and Compression.

Name of Candidate: Subash Yalamarthy
Master of Science in Civil Engineering.

Thesis and Abstract Approved:

C.T. Thomas Hsu, Ph.D., Associate Professor, Department of Civil and Environmental Engineering. Date

Signatures of other members of the thesis

Date

VITA

Name: Subash Yalamarthy

Degree and date to be conferred: MSCE, 1984.

Secondary education: All Saints High School, Hyderabad, India.

Institutions attended	Dates	Degree	Date of Degree
Jawaharlalal Nehru Technological University. Hyderabad, India.	5/77-5/82	B.Tech	May 1982.
New Jersey Institute of Technology, Newark, N.J., U.S.A	9/82-5/84	MSCE	May 1984.

Major: Civil Engineering.

ABSTRACT

Title of Thesis: Behavior of Thin-Walled Channel Shaped Concrete Columns under Combined Biaxial Bending and Compression.

Subash Yalamarthy, Master of Science in Civil Engineering, 1983.

Thesis directed by: Dr. C.T. Thomas Hsu, Associate Professor of Civil Engineering.

Next to rectangular, circular and L shapes, Channel section may be the most frequently encountered reinforced concrete columns since they can be used as box wall for elevators. Nevertheless, information about the load deformation behavior is not generally available to structural engineers. Most of the investigations have been emphasized on the ultimate strength of column sections under combined biaxial bending and axial compression and the resulting interaction surface. No attention is paid to load deformation behavior.

Current code provisions do not provide adequate quidelines for assessing the strength and ductility of biaxially-loaded reinforced concrete columns. Therefore, this investigation is aimed at an experimental and analytical study of the behavior of biaxially-loaded channel-shaped short columns as the applied load is increased monotonically from zero to failure.

For the test purpose four reinforced concrete Channel-shaped columns of nearly half the size of the true specimens were casted and tested till failure. Moment-Curvature and Load Deflection curves obtained from testing channel section were compared with the results from a computer program developed by Hsu[1] and were found to be in excellent agreement. In addition a computer program was developed to calculate the ultimate flexural capacity of cracked arbitrary concrete sections under axial load and biaxial bending based on the Brondum-Nielsen's paper.

Blank Page

TO

MY PARENTS.

ACKNOWLEDGEMENTS

I wish to express my deep gratitude to Dr. C.T. Thomas Hsu who contributed to the completion of this work through his professional support, assistance and encouragement.

I thank Dr. Methi Wecheratana for his valuable suggestions and help throughout the project.

I wish to thank Mr. Amar Shah, Mr. Tony Nader, Mr. Gabriel Hanoush, Mr. Shashin Parikh and Mr. Nithin Kumar Patel for the help extended during casting and testing of specimens.

Special thanks go to my friend Mr. Mahesh R. Taskar whose careful reading of the final draft led to many changes on both a technical and pedagogical level.

TABLE OF CONTENTS

LIST OF TABLES

LIST OF FIGURES

LIST OF FIGURES (Continued)

LIST OF FIGURES (Continued)

LIST OF NOTATIONS

a	- Intercept of Neutral Axis on X-axis
A_c	- Active Concrete Compression Zone Area
a_i	- Area of element i
a_k	- Area of element k
A_i	- Cross Sectional Area of an Individual Reinforcing bar
e_x	- Eccentricity along x axis
e_y	- Eccentricity along y axis
E_c	- Maximum Compressive Concrete Strain
E_k	- Strain in element k
E_s	- Young's Modulus of Elasticity for Steel
f'_c	- Ultimate Strength of Concrete
k	- Element Number
kd	- distance from maximum compressive concrete strain to the neutral axis
l	- total length of column
l'	- Effective length of column
M_{nx}	- $P_n e_y$: Nominal moment in x-direction
M_{ny}	- $P_n e_x$: Nominal moment in y-direction
M_{ox}	- M_{nx} capacity at axial load P_n when M_{ny} is zero
M_{oy}	- M_{ny} capacity at axial load P_n when M_{nx} is zero
M_{ult}	- moment at failure
M_x	- bending moment about x-axis
M_y	- bending moment about y-axis

LIST OF NOTATIONS (Continued)

P - axial load

s - spacing of lateral reinforcement

ϕ - Curvature

ϕ_x - Curvature produced due to bending moment M_x

ϕ_y - Curvature produced due to bending moment M_y

δ_x - deflection in the x-direction

δ_y - deflection in the y-direction

N_u - Ultimate normal force

ε_s - Strain in reinforcing steel

ε_{cu} - Maximum concrete compressive strain

f_{cd} - Ultimate Strength of Concrete

f_{yd} - Yield Strength of steel reinforcement

σ_s - Steel tensile stress

σ_c - Concrete Compressive Stress

CHAPTER 1.

A) INTRODUCTION

Most investigations on the behaviour of concrete under axial compression and biaxial stresses have been primarily concerned with the determination of the ultimate strength of concrete under combined stress and relatively few studies have been presented on the deformational characteristics of concrete subject to biaxial bending.

However, in recent years important developments have been made in the philosophy of structural design. These have been embodied in new codes of practice such as Cp110 which require a structure to be analyzed for compliance with states of serviceability as well as ultimate strength. To satisfy these requirements; information is needed regarding the behavior of concrete under biaxial states of stress throughout the entire loading regime up to ultimate. Comprehensive research work for obtaining such information has been carried out only under uniaxial compression at both the structural and the phenemenological levels.

The investigation, forming the basis of this topic, extends the above work to regimes of biaxial loading. The prime object of this program is to investigate the full range of column behavior, deformation characteristics and moment curvature relationship subjected to biaxial-loading.

The study emphasizes on reinforced concrete columns of channel-shaped cross sections only. Four reinforced concrete channel-shaped columns were tested till failure. By measuring column curvatures, reactions and deformations the moment curvature relationship for a constant axial load was experimentally measured. The moment curvature relationship obtained experimentally was then compared with that obtained from the computer program developed by Hsu[1], on the basis of static equilibrium, where as the stress-strain curves and strain compatability requirements across the column cross sections were among the input variables. A modification of Newton Raphson numerical method was used to achieve the above computation procedures.

B) DESIGN CRITERIA:

Design criteria for eccentrically loaded concrete columns during the last few decades have evolved from allowable stress limits for presumably elastic members toward strength limits that recognize inelastic material response before maximum strength is achieved. Early recognition that compression stress limits at the extreme fibers of concrete cross sections produced unacceptably low estimates of allowable load preceded the adoption of a strength formulation of an allowable stress for the design of non-slender axially loaded columns. Analysis for flexure in addition to thrust continued to require an elastic analysis of the heterogeneous cross sections.

The application of strength criteria as a basis for designing concrete columns would be more complex analytically than the presently available maximum elastic strain and allowable stress block for concrete at ultimate. A constant ultimate stress equal to 85 per cent of the cylinder strength f'_c on a compression zone extending from the extreme fiber 85 per cent of the depth to a neutral axis made strength analysis of columns no more difficult than the allowable stress analysis had been. Under biaxially eccentric loading conditions the use of the rectangular stress block for concrete at ultimate made the strength analysis less complex than the elastic stress analysis.

C) <u>DESIGN PRACTICE:</u>

Almost all columns that support bridges must be designed to resist load combinations that create significant amounts of biaxial bending, but biaxial bending is rarely a critical concern for the design of columns in buildings. Even though every column in every building resists biaxially eccentric thrust most of the time, the limit loading conditions that serve as a basis for structural design are derived from an analysis of frames in the planes in which the principal axes of columns are constructed. Column design moments are largest when live load exists in the bay adjacent to a column only in the direction of maximum moment. Only at the exterior corner of a building does maximum skew bending occur under the same loading that creates maximum moment about each principal axis. The type of framing sometimes eliminates significant skew bending possibilities even at corner columns of buildings.

The ACI Building Code and the AASHTO criteria explicitly recognize the use of the rectangular stress block and the ultimate compressive strain of 0.003 for concrete for strength analysis. More sophisticated representations of the stress strain behavior of concrete are permitted, but only the rectangular stress block is used for the derivation of design aids that are readily available. The design aids are applicable for the strength design of cross sections, presumably after moment magnifiers from slenderness effects have been investigated for the secondary moments acting seperately about each principal axis.

Rectangular cross section capacity is derived from analytical representations of an interaction surface for which thrust capacity is the vertical abscissa and bending capacities about each principal axis are horizontal ordinates. Contours at constant thrust have been described as an elliptic function of the ratios between moment components and moment capacities about each principal axis in the form

$$\left(\frac{M_{nx}}{M_{ox}}\right)^n + \left(\frac{M_{ny}}{M_{oy}}\right)^n = 1.0 \quad \ldots\ldots\ldots\ldots\ldots (1)$$

The magnitude of the exponent 'n' has an upper limit value of 2 when thrust equals the squash load P_o, and the magnitude of 'n' decreases to reflect variables such as the reinforcement ratio, the ratio between the short side and the long side of the rectangle, and the ratio between concrete strength and steel yield strength (f'_c / f_y).

The form of Eq. (1) is convenient, but the apparent precision of accommodating numerous parameters is not appropriate for the real accuracy of the equation. The design aids for determining the exponent 'n' were derived from computer programs that used the rectangular stress block and a limit strain of concrete at ultimate load.

A direct formulation of mathematical expressions for ultimate loads and moments, as is possible for columns eccentrically loaded with respect to one principal axis is virtually impossible.

Even for the simpler case of an eccentrically loaded column, use of the available formulas is restricted to particular position of the steel, i.e. all the steel being concentrated in opposite faces. If the bars are distributed among all faces, the ultimate load can be determined only by a process of trial and error.

The methods available for the design of biaxially loaded columns are: (1) trial and error procedure, and (2) determination of ultimate loads from failure surfaces in columns.

Whitney and Cohen[16] first outlined a successive approximation method. Other investigators later invariably followed the same procedure, adopting some simplifying assumptions to facilitate computation. (see Fig. 1.1).

Recently published methods are based on the concept of failure surfaces in columns. Pannell[17] has shown that the equivalent uniaxial moment M_{uxo} of the radial moment M_u corresponding to any ultimate load P_u can be determined with the aid of the parameters N, the deviation factor and $\emptyset$, the curvature the ratio of M_{ux}/M_{uy}. The theoretical load corresponding to the calculated uniaxial moment is then determined from the major axis interaction diagram.

This procedure, namely, determining the load from the moments, is likely to give rise to possible errors in the estimation of the ultimate load. This is especially the case when the failure is controlled by tension and the calculated equivalent uniaxial moment is nearly equal. In such cases, as seen from the interaction diagram(Fig.1.2) the load falls rapidly for little change in the moment at the onset of tension failure condition.

Of the two methods proposed by Bresler[18] the equation

$$\frac{1}{P_i} = \frac{1}{P_{ux}} + \frac{1}{P_{uy}} + \frac{1}{P_o}$$

is simple and easy to apply. This equation, though exact for materials obeying Hooke's law, gives surprisingly satisfactory results when applied to concrete.

Few analysis and test results have been published on biaxial bending theory and experimentation for channel shaped columns. Among them the theory of Marin[19] and Presley and Park[20](see Fig.1.2) have limited application as they pertain to ultimate strengths of channel shaped reinforced concrete columns. More recently Chidambarrao[21] has presented test results for several channel columns. In these tests, the maximum implied eccentricity ratio is seen to be small and the thicknesses of web and flange of channel section are larger than the present column specimens.

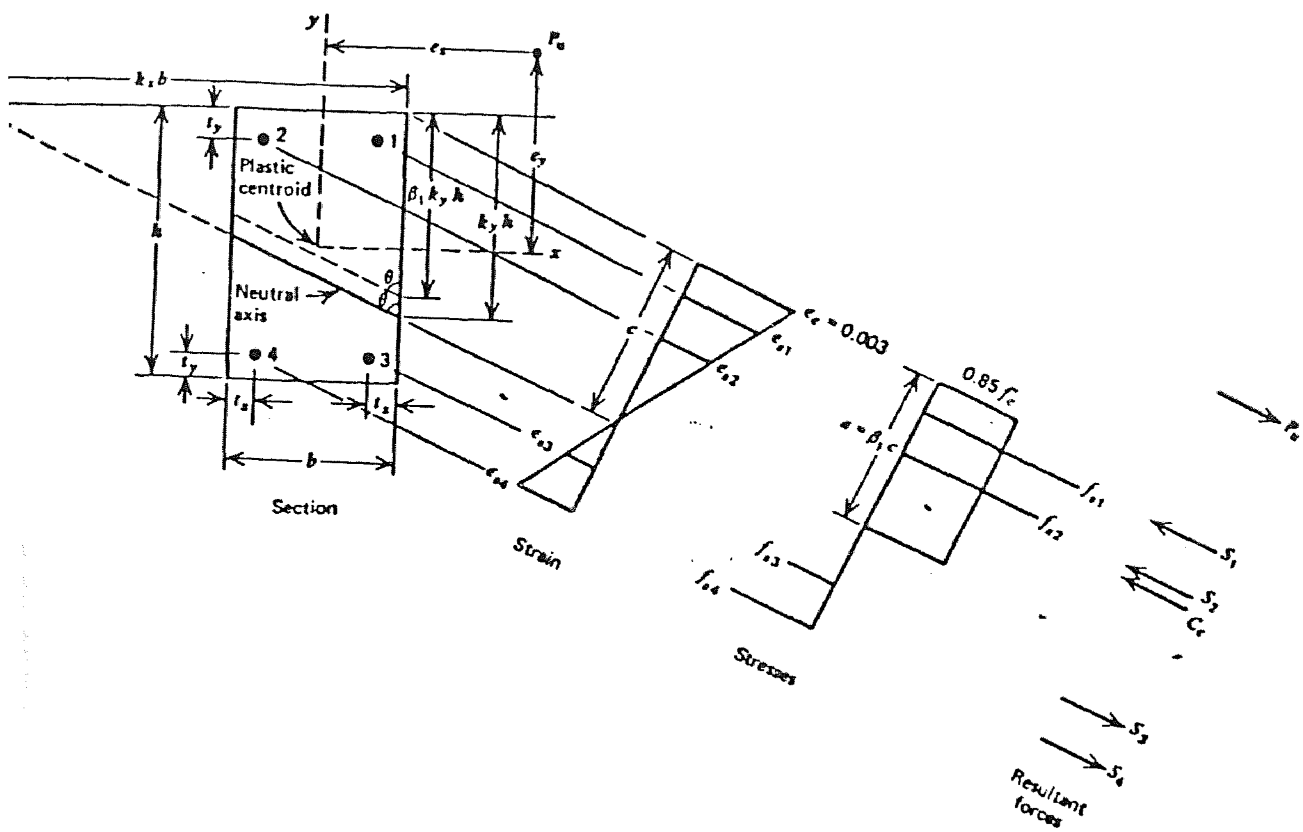

FIGURE 1.1 COLUMN SECTION WITH BIAXIAL BENDING

AT THE ULTIMATE LOAD

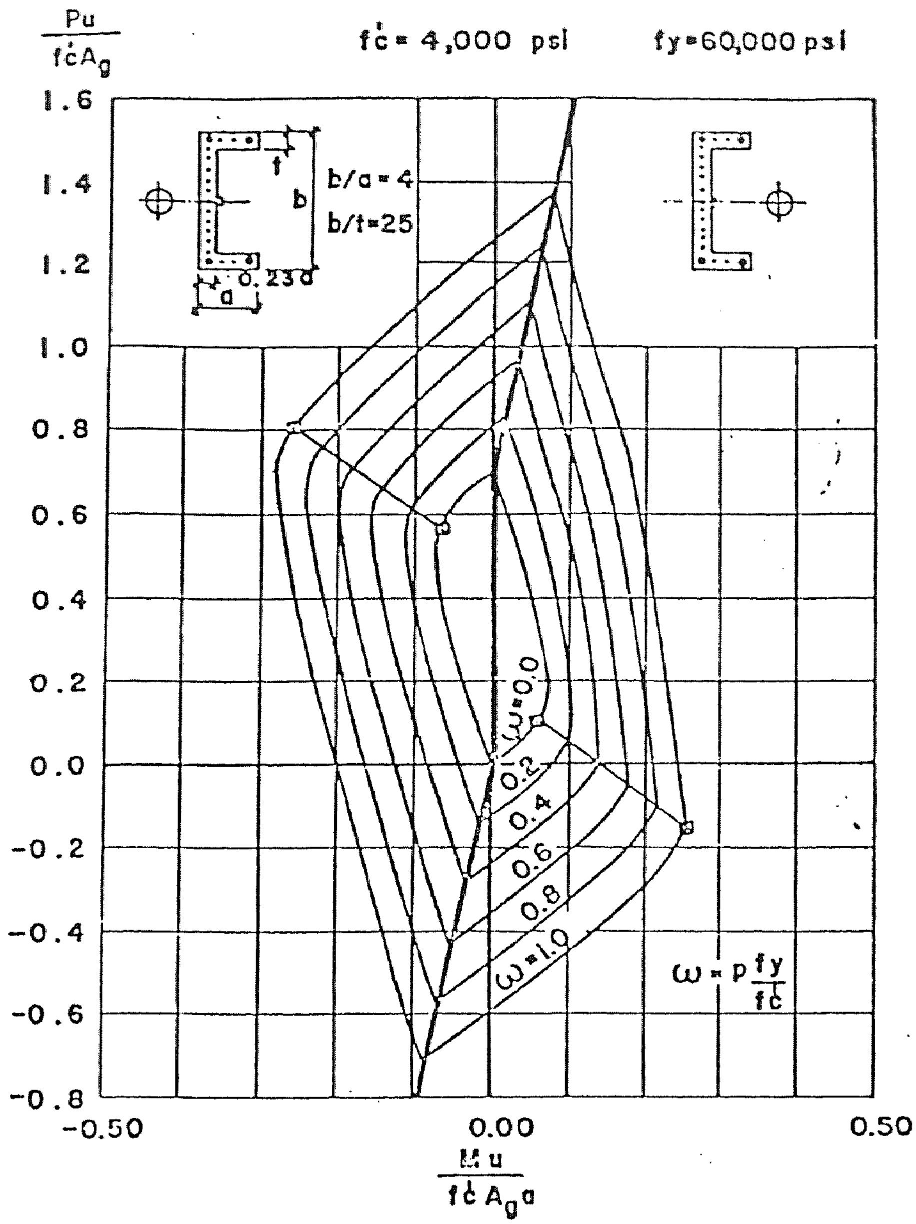

FIG 1.2 INTERACTION DIAGRAM FOR "C" CROSS SECTION

CHAPTER II TEST PROGRAM

A) DETAILS OF TEST SPECIMENS

Four reinforced concrete channel shaped columns of nearly half the size of the true specimen were tested till failure. The specimen has a channel section with 7.5 in. breadth, 15 in. width and 1.5 in. thick as shown in figure (5.1). The columns were designed as short columns and were each six feet long. The six feet length of column consisted of two end brackets of length one half feet. Proper care was taken in designing the column and column bracket portion which conform to current code practice.

Each concrete unit had eighteen number #3 longitudinal bars of grade 60. The longitudinal bars were held in proper position by using steel ties of grade 60. The arrangement of longitudinal bars in the section is of interest because it has been shown that the presence of well tied intermediate column bars between the corner bars significantly improves the confinement of the concrete.[14] The center to center spacing of longitudinal bars across the section was determined such that the spacing did not exceed one third of the section dimension in that direction or 8.0 in whichever was larger.

All transverse reinforcement was from plain round bars and the bars were anchored normally by a 135 degree bend around a longitudinal bar, plus an extension beyond the bend, atleast eight tie bar diameters, embeded in the concrete core. The spacing of transverse ties was reduced by one half for the 15 inches of bracket portion at each end of the test units to provide extra confinement and insure that failure occured in the four and half feet long central region.

B) MATERIAL PROPERTIES

Type III Portland Cement(High early strength) was used. Standard river washed sand was employed as fine aggregate. The water cement ratio varied from 0.70 to 0.80 by weight and the aggregate(sand) cement ratio was 3.2. The slump was held between 2in. and 3in.

C) PROPORTIONING

Cement/Sand : 3.2

Water/cement : 0.7 to 0.8

Dry ingredients were used for all mixes and the proportioning was by weight.

D) CASTING

The test specimens were cast horizontally. For each batch of mixing six control cylinders of size 3in by 6in. were casted and cured in the same way as that of column specimens.

E) INSTRUMENTATION

1. LOADING METHOD: The testing was carried out by using Enerpac 100 ton capacity hydraulic cylinder ram (effective area = 20.63 in.^{2}). The columns were axially loaded and the testing was carried out in horizontal position. The loading stress was directly read through a pressure gauge and the effective load was calculated by multiplying pressure with the effective area of the ram.

2. STRAIN AND CURVATURE MEASUREMENTS: The measurements of strain and curvature were done by the demec gauge method. The strain was calculated from measured deformation, between a pair of demec points, divided by the distance between the two points. The distance between a pair of demec gauges was 6in.

3. DEFLECTION MEASUREMENTS: The measurements of the mid-span deflections were made using Ames dial gauges. A set of dial gauges were used to determine the deflection in both directions X and Y.

CHAPTER III.

TEST PROCEDURE

A) STEEL REINFORCEMENT TESTS:

Random samples of the bars were taken and tested in a Universal testing machine in tension till failure. 480 mm length of test specimens were cut from the #3 bars and punch marks were marked 55 mm apart. The strain measurements were taken using a strain gauge of least count 0.01in. The resulting stress strain curve for the reinforcing steel is shown in Figure.(3.1)

B) CYLINDER TESTS:

Six 3X6 inch (standard size) cylinders were cast for each batch mix of concrete. The cylinders were tested on a 400,000 pound capacity hydraulic testing machine till failure and the ultimate strength of concrete was then calculated.

C) COLUMN TESTS:

The load points were marked on the bracket face and the Demec gauges were glued at the 6 in central portion symmetrically on two adjacent sides of the column specimen. Then the specimen was hoisted into the frame and adjusted such that the load goes through in a straight line from one end to the other, with the exact required eccentricities (see Fig. 3.2 and Fig. 3.3).

A steel plate was placed flat against the bracket face on each end inorder to ensure a uniform distribution of load on the bracket face.

A small initial load was applied to hold the column in proper position and then the initial readings of all demec gauges and dial gauges were taken. The load was then increased in increments of 500 psi. Once the dial gauges came to rest the readings for each load were taken. The load was increased until the failure of the specimen occured and the failure load was recorded. Figure 3.4 and Figure 3.5 illustrate the column specimens after testings. As can be seen, the failure of the column specimens are characterized as compression failure in the flanges.

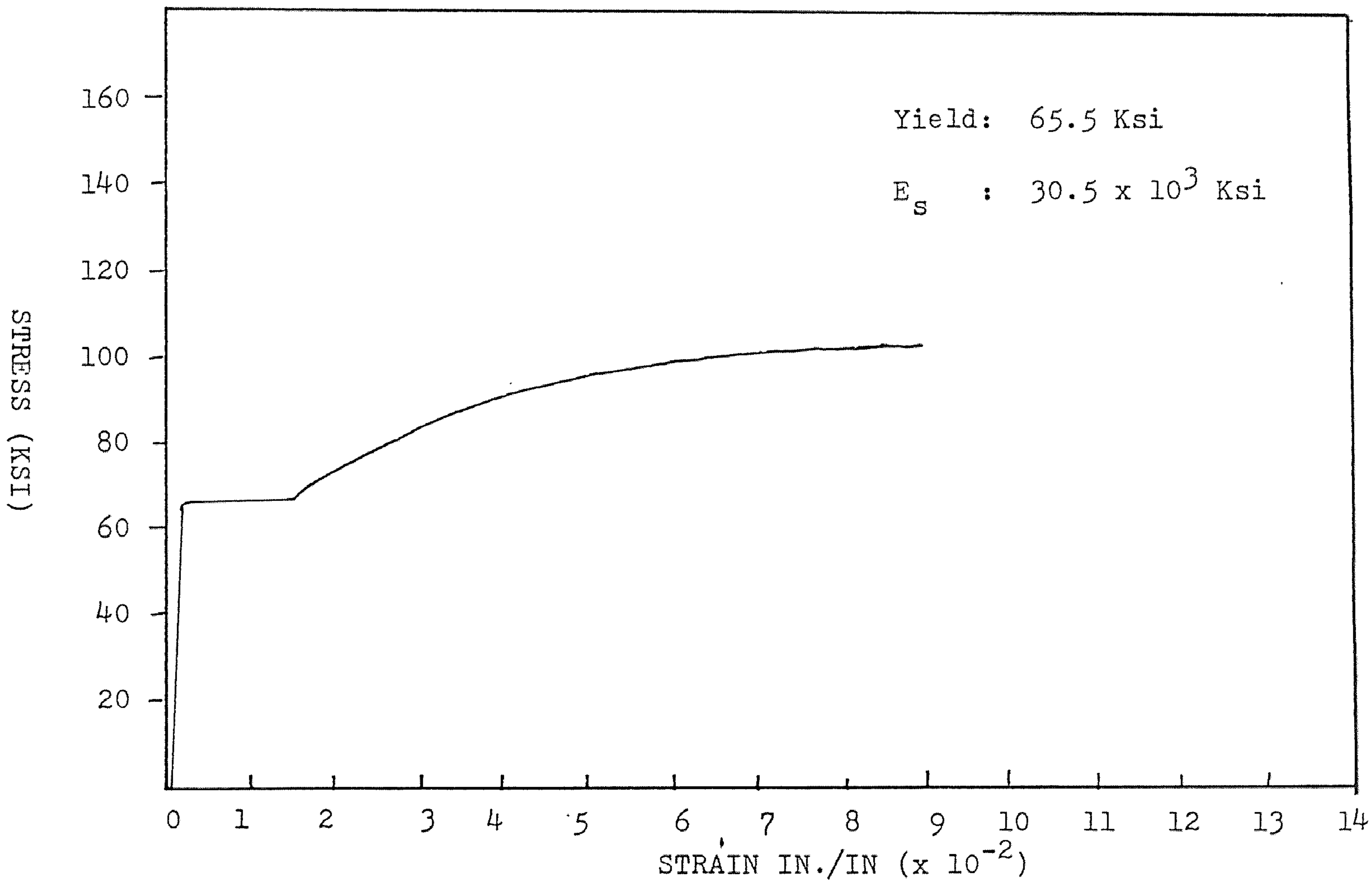

FIGURE 3.1 STRESS STRAIN CURVE FOR STEEL REINFORCEMENT

Fig. 3.2. Testing Frame

Fig. 3.3. Demec Gauge Arrangement

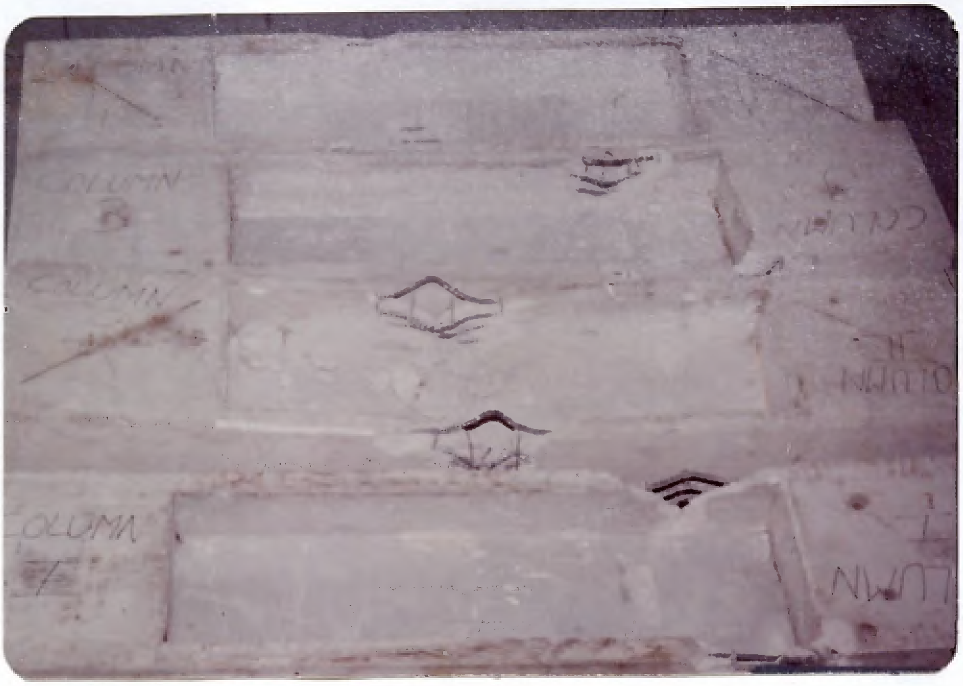

Fig. 3.4. Failure pattern in all Columns

Fig. 3.4. Column after compression failure.

CHAPTER IV

DETERMINATION OF ULTIMATE FLEXURAL CAPACITY OF A CRACKED ARBITRARY CONCRETE SECTIONS UNDER AXIAL LOAD AND BIAXIAL BENDING:-

A computer program to calculate the ultimate flexural capacity of cracked arbitrary concrete sections under axial load and biaxial bending was developed based on the Brondum - Nielsen's[10] paper.

The program has the ability to use any arbitrary concrete cross section with arbitrary reinforcement. Given stress strain relationships for concrete and steel, the program can find the ultimate limit state value of normal force 'N'.

Sign Convention:

Steel tensile stress σ_s and concrete compressive stresses $\sigma_c = f_{cd}$ are taken as positive. Also compressive force is assumed to be positive.

Arbitrary cross section:

An arbitrary cross section loaded by an eccentric axial load N_u is shown in Fig. 4.4, which also illustrates the assumptions regarding cracked cross section, plane strain distribution, stress-strain relationships, etc.

The cross-sectional area of an individual reinforcing bar is denoted A_i and elements of the active concrete compression zone dA_c.

Moment equilibrium with respect to the axes through the normal force N_u and parallel to the arbitrary orthogonal X-and Y-axes, respectively, requires:

$$f_1 = \Sigma(y_i - e)A_i \sigma_{si} - f_{cd}\int(y-e)dA_c = 0 \quad \text{........(1)}$$

$$f_2 = \Sigma(x_i - n)A_i \sigma_{si} - f_{cd}\int(x-n)dA_c = 0 \quad \text{........(2)}$$

Equilibrium of axial force components requires:

$$N_u = f_{cd}A_c - \Sigma A_i \sigma_{si} \qquad \text{........(2a)}$$

If the origin is loacated at the point with maximum concrete compressive strain ε_{cu} (as in Fig.4.5), then the plane strain distribution requires:

$$\varepsilon_s = \varepsilon_{cu}\left(\frac{x}{a} \; \frac{y}{h} - 1\right) \qquad \text{........(2b)}$$

The stress-strain relationship for the steel can be expressed as follows:

$$|\varepsilon_s| < \varepsilon_o : \quad \sigma_s = E_s \cdot \varepsilon_s \qquad \text{........(2c)}$$

$$|\varepsilon_s| \geqslant \varepsilon_o : \quad \sigma_s = \varepsilon_s |\varepsilon_s|^{-1} \cdot f_{yd} \qquad \text{........(2d)}$$

The value of the maximum concrete compressive strain ε_{cu} is assumed to be determined by code specifications. The main problem is thus limited to determination of the neutral axis, i.e., the values of a and h.

The non-linear equations 1 & 2 can be solved by a two dimensional, root finding algorithm. The nonlinear equations can, for instance, be solved by a two dimensional Newton Raphson iteration using finite differences in lieu of the partial derivatives.

Iteration Step No. i yields:

$$a_{i+1} = a_i - D^{-1}(f_1.df_2/dh - f_2.df_1/dh)_i \qquad \text{........(2e)}$$

$$h_{i+1} = h_i - D^{-1}(f_2.df_1/da - f_1.df_2/da)_i \qquad \text{........(2f)}$$

with the notation:

$$D_i = (df_1/da.df_2/dh - df_1/dh.df_2/da)_i \qquad \text{........(2g)}$$

The highlight of this program is that it can shift automatically between triangular, trapezoidal and pentagonal compression zones as the iterations adjust the estimated location of the neutral axis.

$$\chi = 1 - b/n.a \qquad \text{..........(3)}$$

$$\psi = 1 - t/n.h \qquad \text{..........(4)}$$

Pentagonal Compression Zone

For the case of a pentagonal compression zone the following relations apply:

$$A_c = 1/2\ n^2ah(1-\chi^2-\psi^2) \qquad \text{........(5)}$$

$$\int YdA_c = 1/6\ n^3ah^2[1-\chi^3-\psi^3(3-2\psi)] \qquad \text{........(6)}$$

$$\int XdA_c = 1/6\ n^3a^2h[1-\psi^3-\chi^2(3-2\chi)] \qquad \text{........(7)}$$

Trapezoidal or triangular compression zone

It will be seen from Fig.4.5that the compression zone for $\eta a<b$, i.e., ($\chi<0$) or for $\eta h<t$, i.e., ($\psi<0$) becomes trapezoidal and for negative values of both χ and ψ, triangular, Eq.(5) through (7), consequently also cover these cases if the following equations are substituted for Eq. (3) and (4);

$$\chi = 1- b/n.a \nless 0$$

$$\psi = 1- t/n.h \nless 0$$

The symbol $\nless$ indicates that if the expression to the left of the symbol leads to a negative value, then zero should be substituted for χ or ψ. The computer program is thus arranged to shift automatically between these possible shapes of compression zone, which cover a large percentage of cases encountered in practice.

Fig.(4.6) shows the flowchart for the computer program.

<u>NUMERICAL EXAMPLE</u>

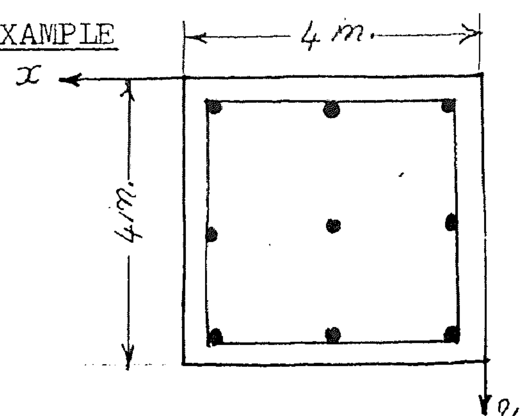

Fig. (4.0)

The cross section shown in Fig.(4.0) is provided with nine reinforcing bars. The cross sectional area of each reinforcing bar is 0.0001979 m^2.

The following quantities are given:

$$f_{cd} = 18.466 \text{ MPa}$$

$$\varepsilon_{cu} = 0.0035$$

$$\eta = 0.70$$

$$f_{yd} = 322.69 \text{ Mpa}$$

$$E_s = 2.0 \times 10^5 \text{ Mpa}$$

$$a = 0.2744 \text{ m (estimated)}$$

$$h = 0.2744 \text{ m (estimated)}$$

The above cross section is one among several test specimens tested by Ramamurthy[22] at Indian Institute of Technology. The computer program developed was used to analyse the experimental results obtained by Ramamurthy[22] and it was found to be in excellent agreement. These results are shown in appendix II.

The above computer method can be used to calculate the ultimate strength capacity for a given section. However it does not account for the determination of both strength and deformation for an arbitrary corss section. In the present analytical study the computer method developed by Hsu[1] was used to compare with the experimental results of the present study. Fig. 4.1 shows a typical load deformation result from Hsu's[1] method. Fig. 4.2 presents an arbitrary section under combined biaxial bending and axial load, the section will be divided into several small elements, for analytical purpose. Fig. 4.3 illustrates typical stress-strain curves for concrete and reinforcing steel to be used in Hsu's[1] program. More details of Hsu's[1] analysis and computer method can be found in Reference 1.

BASIC ASSUMPTIONS:

The following assumptions have been made in this theoretical analysis:

(1) The bending moments are applied about the principal axis.

(2) Plane sections remain plane.

(3) The longitudinal stress at a point is a function only of the longitudinal strain at that point. The effect of creep and shrinkage are ignored.

(4) The stress-strain curves for the materials used are known.

(5) Strain reversal does not occur.

(6) The effect of deformation due to shear and torsion and impact effects are negligible.

(7) The section does not buckle before the ultimate load is attained.

(8) Perfect bond exists between the concrete and the reinforcing steel.

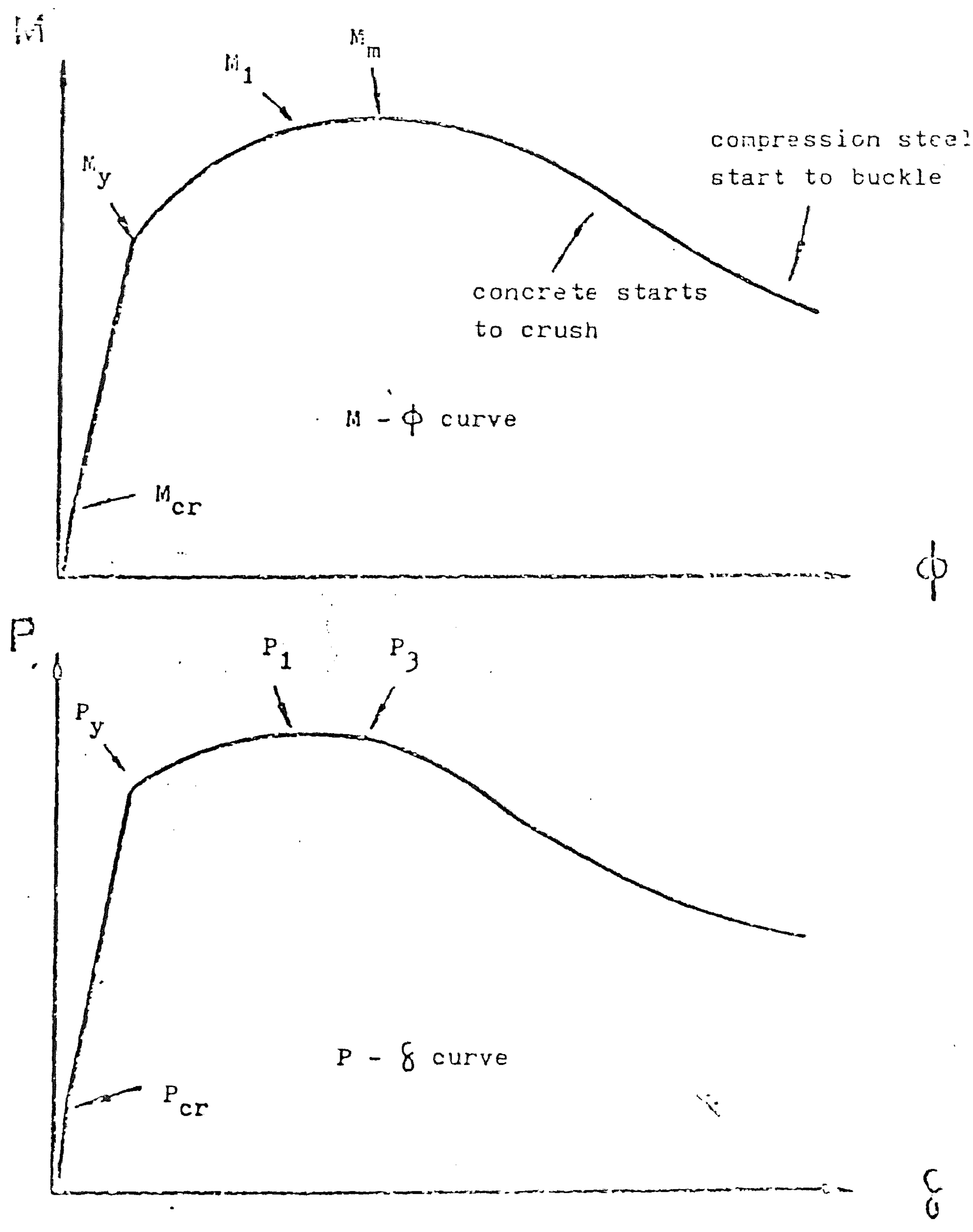

G. 4.1 TYPICAL RELATIONSHIP BETWEEN MOMENT-CURVATURE AND LOAD-DEFLECTION CURVES FOR SHORT COLUMNS

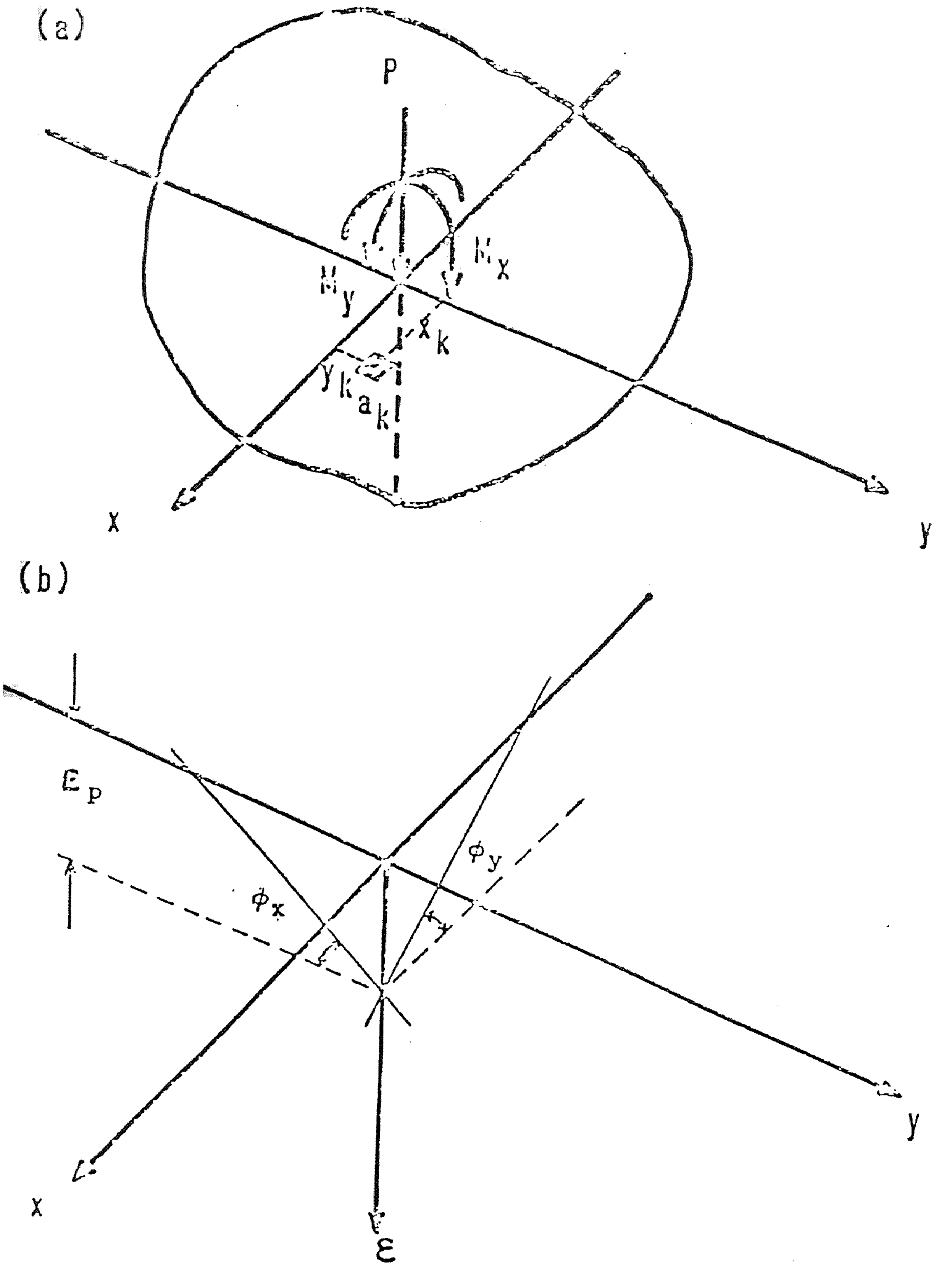

IG 4 2 IDEALIZATION OF A CROSS-SECTION SUBJECTED TO BIAXIAL BENDING AND AXIAL LOAD

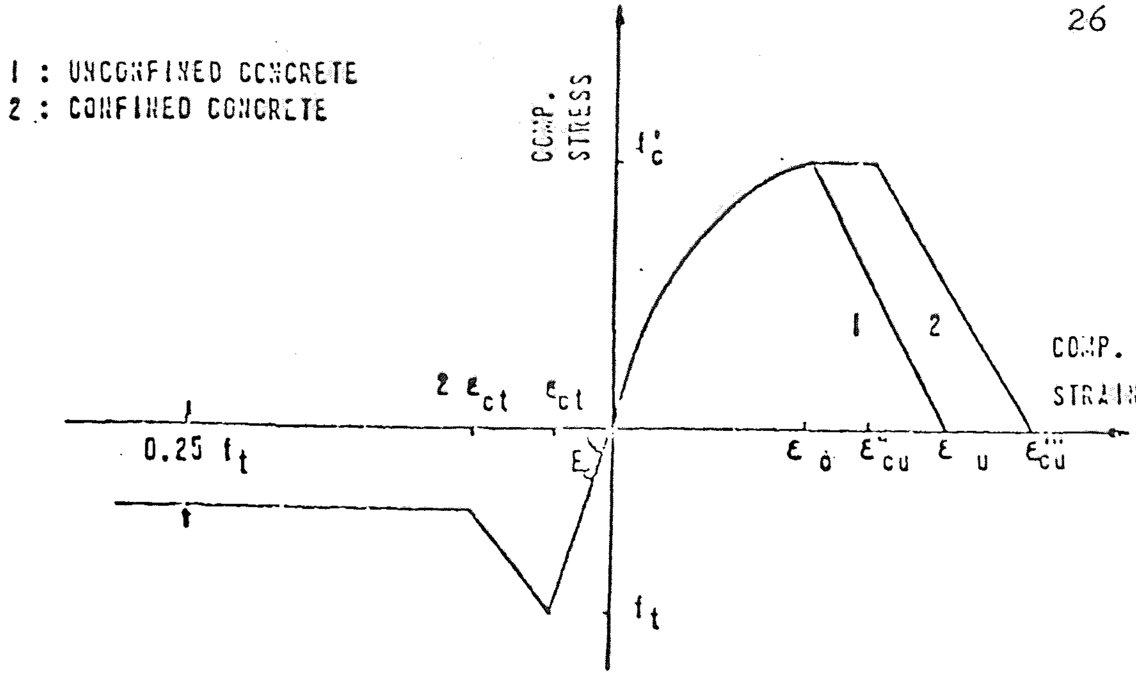

FIG. 4.3.a IDEALIZED STRESS-STRAIN CURVES FOR CONCRETE

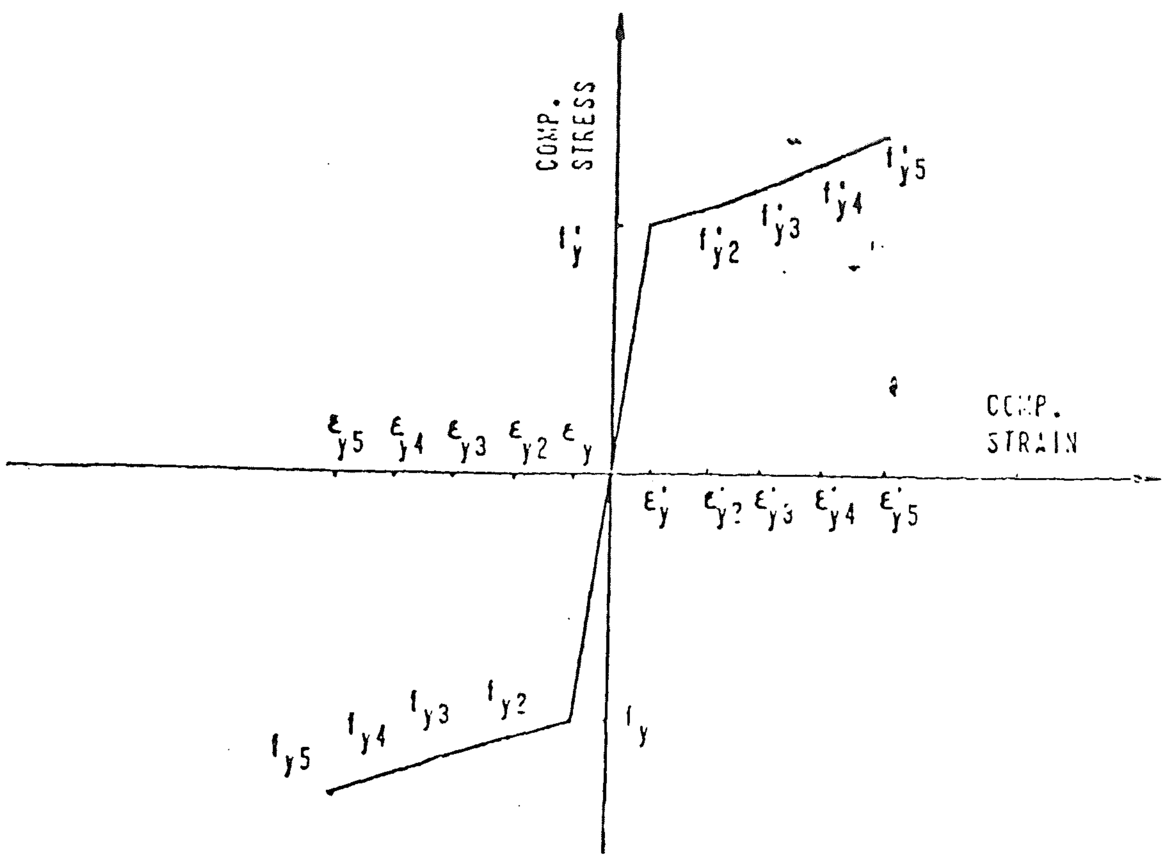

FIG 4.3.b IDEALIZED STRESS-STRAIN CURVE FOR STEEL

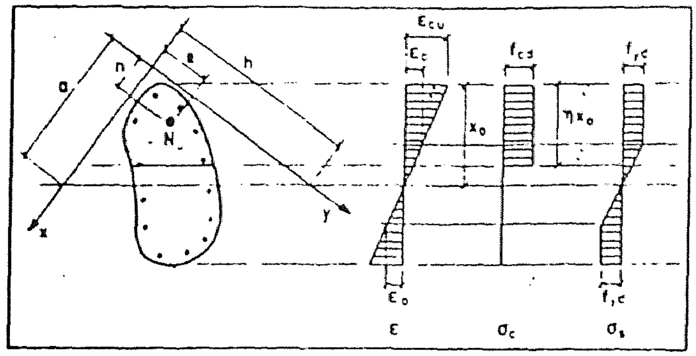

Fig. (4.4) Cracked Arbitrary Cross Section loaded by an eccentric Axial Load.

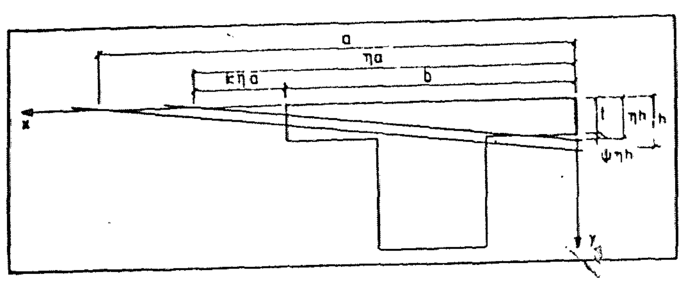

Fig. (4.5) Pentagonal Compression zone

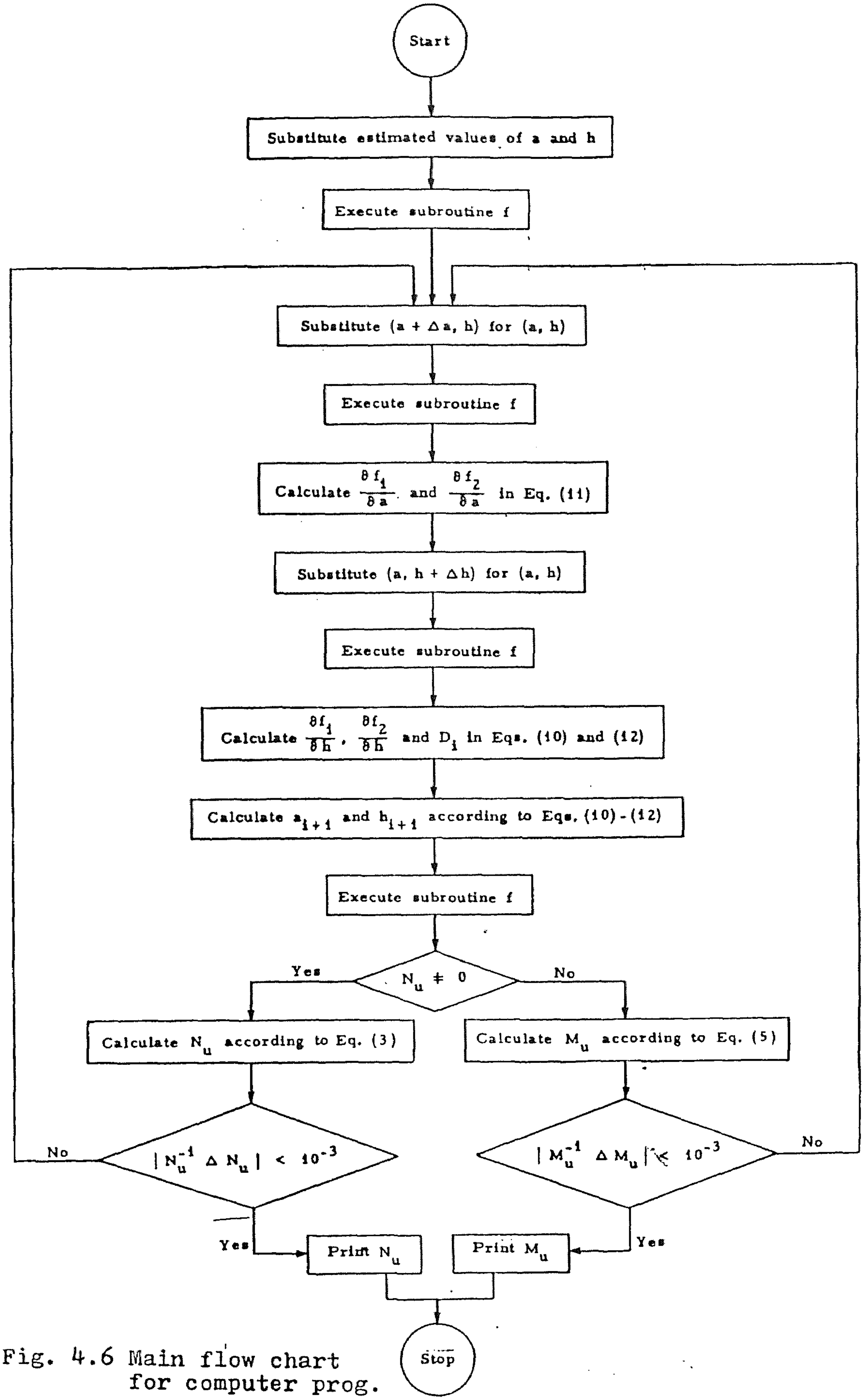

Fig. 4.6 Main flow chart for computer prog.

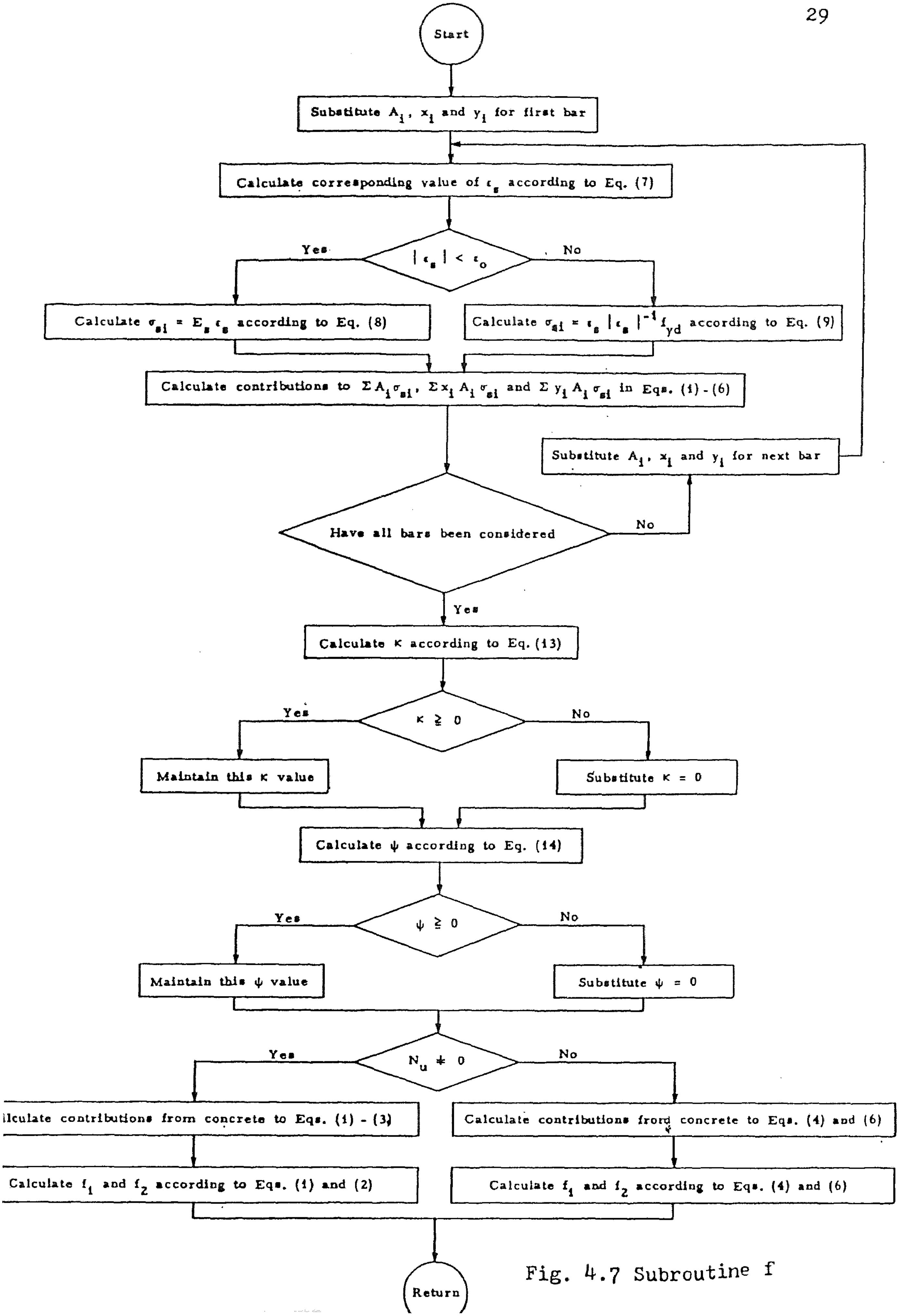

Fig. 4.7 Subroutine f

CHAPTER 5.

ANALYSIS OF TEST RESULTS

Four reinforced channel shaped column sections were tested till failure. Strains and deflection at various loads were determined from demec gauges and dial gauges readings respectievely. Then the experimental results were compared with the results obtained by using a computer program developed by Hsu[1]. For simplicity and convenience of comparison, the experimental and theoretical results are plotted on the same graph and the detailed step by step calculations are only shown for column #1.

1. LOAD DEFLECTION CURVES: Since the computer program developed by Hsu[1] does not take into consideration the secondary moments that are developed, the axial load P_1 was reduced to an equivalent axial load P_3 by using the equations developed by Hsu and Mirza[23].

Hsu and Mirza[23] proposed the approximate equations using the well modified moment-area theorem to evaluate the central deflections and therby equivalent load P_3 due to secondary bending moment.

The equations are as follows:

$$\delta_{2x} = \phi_y . l^2/8 \qquad \ldots\ldots\ldots\ldots\ldots\ldots (1)$$

$$\delta_{2y} = \phi_x . l^2/8 \qquad \ldots\ldots\ldots\ldots\ldots\ldots (2)$$

and $\delta_{2x} - \delta_{1x} = \phi_y l'^2/8$ .... (3)

$\delta_{2y} - \delta_{1y} = \phi_x . l'^2/8$ .... (4)

Where the behaviour of the bracket region in bending is assumed to be the same as the rest of the column sections.

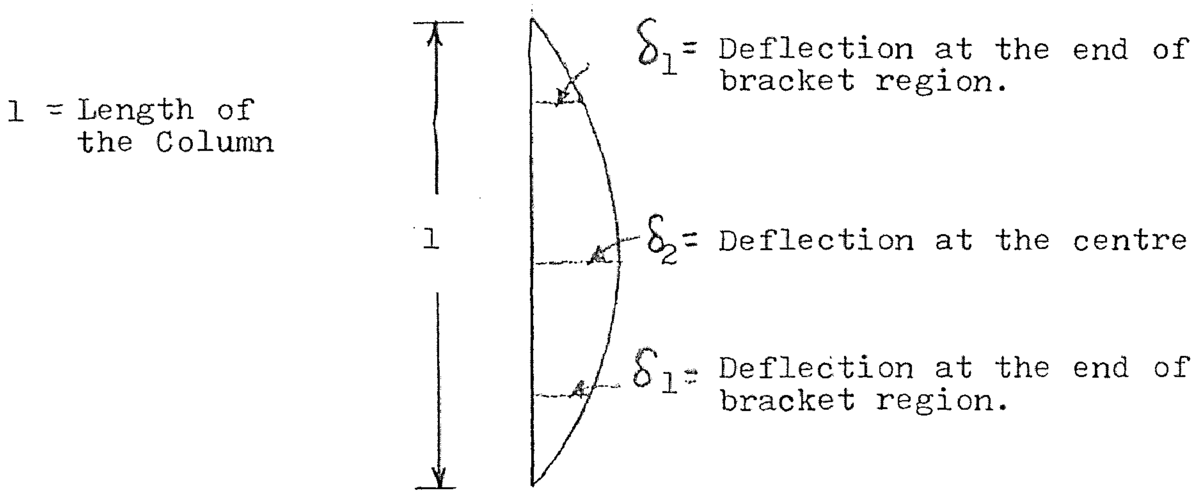

The equivalent axial load P_3 is calculated by P_1, together with the factors which relate to the effect of the mid span deflection. The equations are as follows:

$$P_3 = \frac{P_1(e_x^2 + e_y^2)^{0.5}}{\left\{[e_x + (\delta_{2y} - \delta_{1y})]^2 + [e_y + (\delta_{2x} - \delta_{1x})]^2\right\}^{0.5}} \quad \ldots.(5)$$

Neglecting δ_{1y} and δ_{1x} we have

Where e_x and e_y are the eccentricities along x and y axis respectively.

$$P_3 = \frac{P_1(e_x^2 + e_y^2)^{0.5}}{[(e_x + \delta_{2y})^2 + (e_y + \delta_{2x})^2]^{0.5}} \quad \ldots.(6)$$

Once the axial load P_3 was calculated, a graphical plot was made with axial load P_3 on the Y-axis and deflection on X-axis. On the same graph the experimental load deflection curve was also plotted. Two graphs have been plotted for each specimen: Load deflection curve in the X-direction and load deflection curve in the Y-direction. The complete calculations for column number 1 load deflection, are shown in tables 5.1.a, 5.1.b and 5.1.c.

2. MOMENT CURVATURE RELATIONSHIP: The strain measurements were made by using demec gauges. The distance between a pair of demec gauge was 6 in. with a possible error of 0.05 inches. For simplicity this gauge was assumed to be exactly 6 in. Knowing the change in length between the demec gauges, the strain was computed at each demec gauge level, by using the formula $\Delta l/l$.

The strains at various demec gauge levels were found for all loads and then a plot of strain vs. distance was drawn. The strain distribution acrorss the section, both in the x and y direction was calculated for each load. Then for each load the average curvature was found from the following formula:

$$\phi = \epsilon_c/kd \qquad \text{..................(7)}$$

Where ϕ = Curvature

ε_c = Maximum Compressive Concrete Strain (cracked),
kd = distance from this maximum compressive concrete strain to the neutral axis.

The complete calculations are shown for column #1. Table 5.1.d shows the measured values of changes in length between pairs of demec gauges and table 5.1.e shows the strains of concrete surface between demec gauge pairs.

The experimental moment consisted of primary and secondary bending moments and the total moment was calculated by,

$$M_x = P(e_y + \delta_y) \qquad \ldots\ldots\ldots\ldots\ldots(8)$$

$$M_y = P(e_x + \delta_x) \qquad \ldots\ldots\ldots\ldots\ldots(9)$$

The moment thus calculated was plotted against the corresponding curvatures. The values of bending moments and the curvatures are shown in table 5.1. The theoretical and the experimental curves were plotted on the same graph to provide a comparison of the results.

FIG. 5.1.

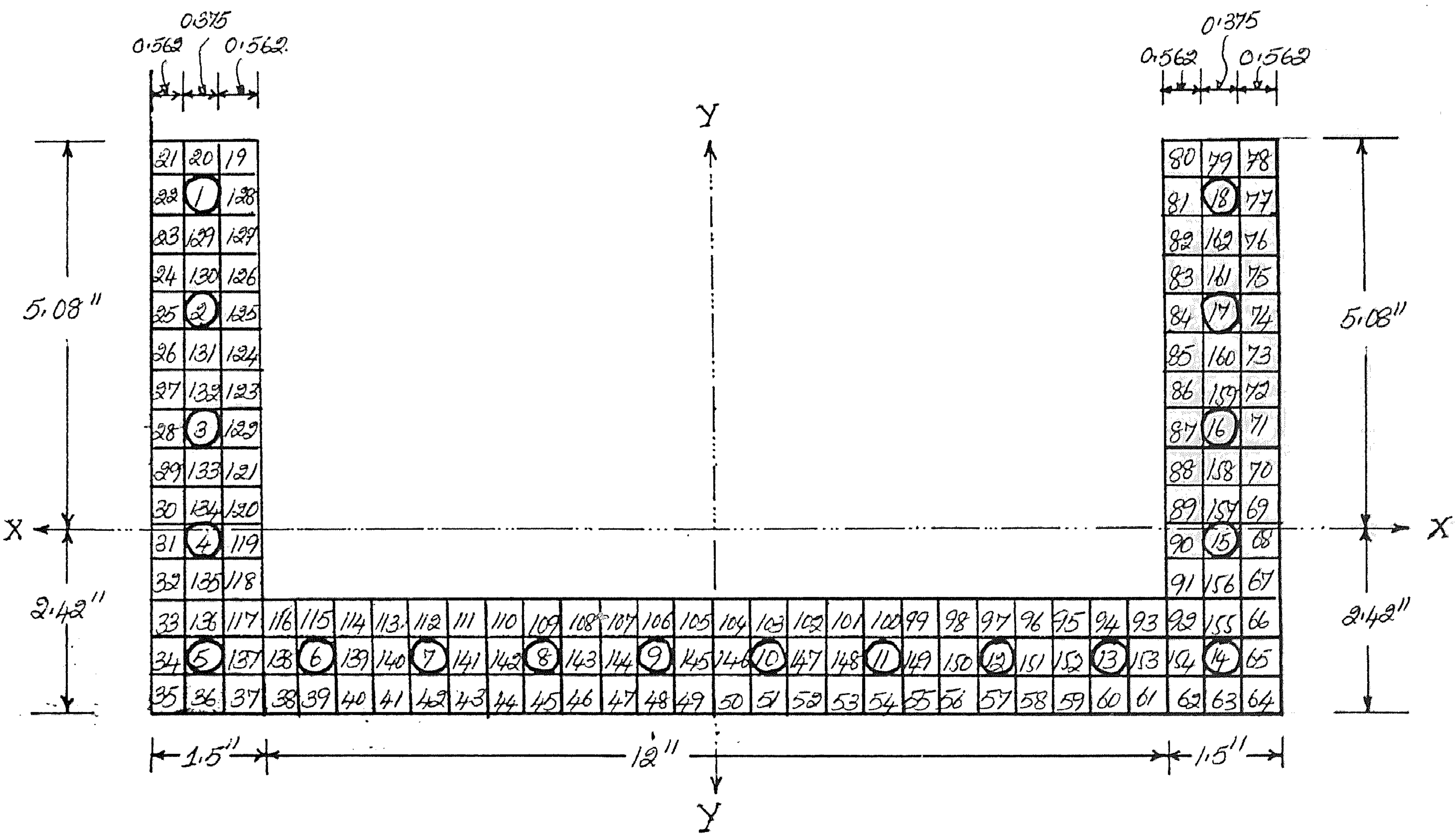

Cross Section Of Column
with 162 Finite Elements.

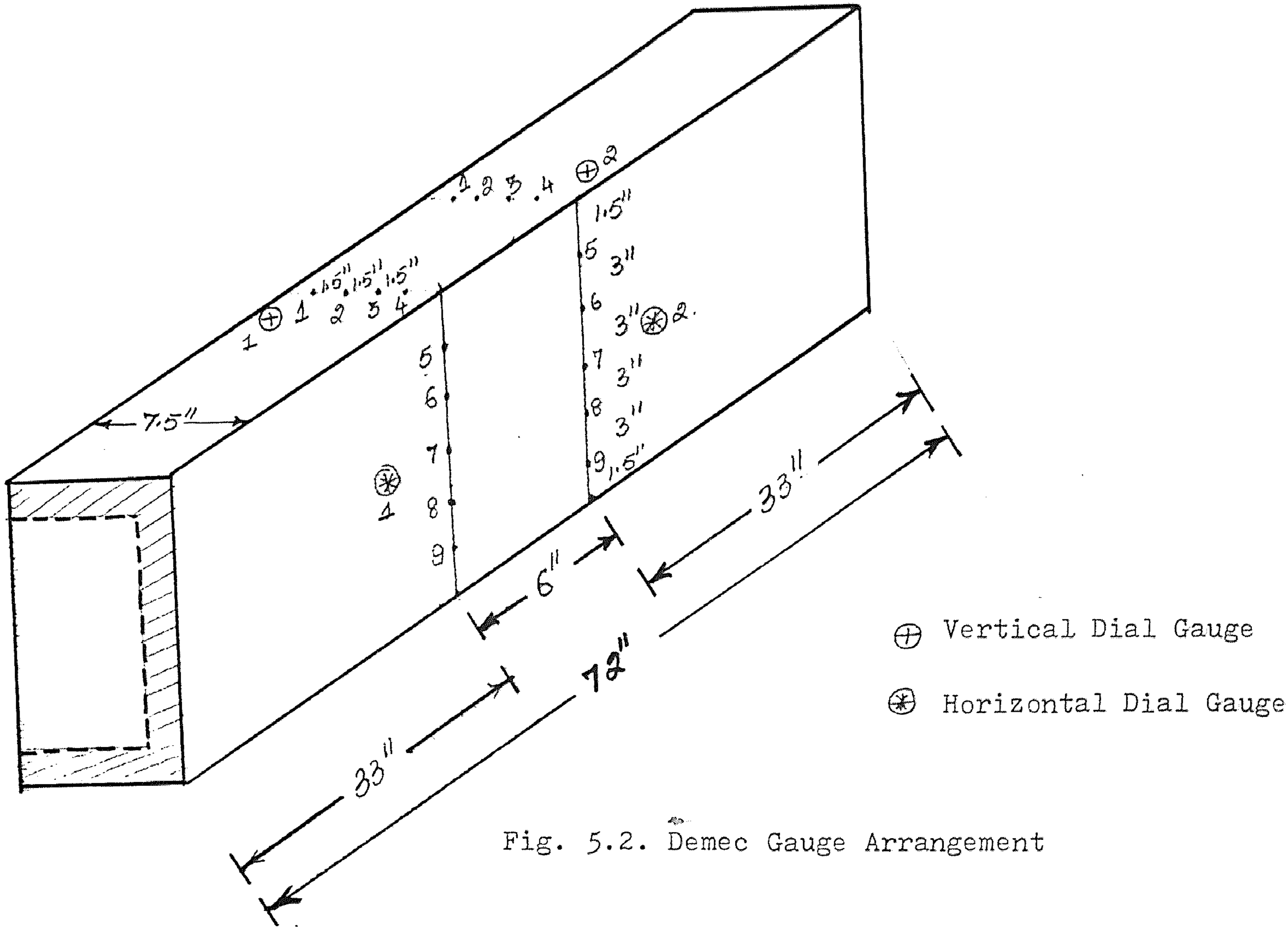

Fig. 5.2. Demec Gauge Arrangement

Table 5.0.

SPECIMEN DETAILS

Column Specimen No.	No. and Size of Bars	f_y (ksi)	A_s. (#1 bar) (in. squared)	S (in.)	f_c' (psi)	e_x (in.)	e_y (in.)
1.	18 #3	65.5	0.1227	3	4232	3.726	2.520
2.	18 #3	65.5	0.1227	3	4232	4.140	2.804
3.	18 #3	65.5	0.1227	3	2964	4.554	3.085
4.	18 #3	65.5	0.1227	3	2964	4.9690	3.370

Table 5.1.a.

LOAD vs. VERTICAL DEFLECTION CALCULATIONS FOR COLUMN #1.

Load (psi)	Load (kips)	Vertical Gauge #1 (inch)	Vertical Gauge #2 (inch)	Vertical Deflection Gauge#1 (inch)	Vertical Deflection Gauge #2 (inch)	Average Vertical Deflection at Mid-Span (inch)
0	0	0.420	0.849	0	0	0
500	10.31	0.415	0.847	0.005	0.001	0.0030
1000	20.63	0.398	0.842	0.022	0.0035	0.0130
1500	30.95	0.382	0.840	0.038	0.0045	0.0213
2000	41.26	0.368	0.831	0.052	0.0090	0.0305
2500	51.58	0.358	0.829	0.062	0.0100	0.0360
3000	61.89	0.347	0.824	0.073	0.0125	0.0428
3500	72.21	0.336	0.818	0.084	0.0155	0.0498
4000	82.52	0.322	0.804	0.098	0.0225	0.0603
4500	92.84	0.307	0.745	0.113	0.0520	0.0825
5000	103.15	0.291	0.728	0.129	0.0605	0.0978
5200	107.28	Failure.				

Table 5.1.b

LOAD vs. HORIZONTAL DEFLECTION CALCULATIONS FOR COLUMN #1.

Load (psi)	Load (kips)	Horizontal Gauge #1 (inch)	Horizontal Gauge #2 (inch)	Horizontal Deflection Gauge #1 (inch)	Horizontal Deflection Gauge #2 (inch)	Average Horizontal Deflection at Mid-Span (inch)
0	0	0.533	0.475	0	0	0
500	10.31	0.534	0.471	0.001	0.004	0.0025
1000	20.63	0.542	0.453	0.009	0.022	0.0155
1500	30.95	0.553	0.431	0.020	0.044	0.0320
2000	41.26	0.558	0.415	0.025	0.060	0.0425
2500	51.58	0.570	0.394	0.037	0.081	0.0590
3000	61.89	0.586	0.368	0.053	0.107	0.0800
3500	72.21	0.494	0.352	0.139	0.123	0.1310
4000	82.52	0.361	0.315	0.172	0.160	0.1660
4500	92.84	0.243	0.161	0.290	0.314	0.3020
5000	103.15	0.139	0.065	0.394	0.410	0.4020
5200	107.28	Failure.				

Table 5.1.c

REDUCED AXIAL LOAD P_3

CALCULATIONS FOR COLUMN #1.

Load P_1 (kips)	e_x (in)	e_y (in)	ϕ_x 1/inch	ϕ_y 1/inch	δ_{2x} (in)	δ_{2y} (in)	Reduced Axial load P_3 (kips)
40.00	3.726	2.520	8.40	2.00	0.0129	0.054	39.58
50.00	3.726	2.520	10.80	2.60	0.0168	0.069	49.47
60.00	3.726	2.520	13.40	3.20	0.0207	0.086	59.01
70.00	3.726	2.520	16.50	4.00	0.0259	0.106	68.58
80.00	3.726	2.520	21.00	5.10	0.0330	0.136	77.95
90.00	3.726	2.520	27.70	6.90	0.0447	0.179	86.97
100.00	3.726	2.520	53.10	12.10	0.0784	0.344	93.80
100.10	3.726	2.520	53.90	12.30	0.0797	0.349	93.75
100.20	3.726	2.520	54.90	12.40	0.0803	0.355	93.70

Table 5.1.d.

MEASURED VALUES OF CHANGES IN LENGTH BETWEEN PAIRS OF DEMEC GAUGES FOR COLUMN #1.

All units are multiplied by a factor of $(x10^{-5})$

Load (psi)	Demec Gauge Pairs 1	2	3	4	5	6	7	8	9
0	1812	1999	2060	1650	394	697	555	985	1360
500	1821	2006	2066	1654	395	698	556	985	1359
1000	1828	2013	2070	1657	398	700	556	985	1359
1500	1841	2022	2078	1663	401	702	558	985	1358
2000	1843	2024	2079	1664	403	703	558	986	1357
2500	1860	2038	2090	1671	405	704	559	986	1356
3000	1878	2053	2102	1678	406	705	559	985	1355
3500	1891	2064	2110	1684	414	710	561	985	1353
4000	1944	2104	2141	1706	415	711	562	984	1352
4500	2013	2161	2183	1734	431	721	566	983	1346
5000	2142	2263	2258	1786	465	742	575	980	1331
5200	Failure.								

Table 5.1.e.

STRAINS OF CONCRETE SURFACE BETWEEN DEMEC GAUGE PAIRS - FOR COLUMN #1.

All units are multiplied by a factor of ($x10^{-5}$)

Load (psi)	1	2	3	4	5	6	7	8	9
0	0	0	0	0	0	0	0	0	0
500	15.40	11.67	10.00	6.67	1.67	1.67	1.67	0	-1.67
1000	26.67	23.33	16.67	11.66	6.67	5.00	1.67	0	-1.67
1500	48.33	38.33	30.00	21.66	11.66	8.33	5.00	0	-3.33
2000	51.67	40.00	31.67	23.33	15.40	10.00	5.00	1.67	-5.00
2500	80.00	65.00	50.00	35.00	18.33	11.66	6.67	1.67	-6.67
3000	110.00	90.00	70.00	46.67	20.00	13.33	6.67	0	-10.00
3500	131.67	108.33	83.33	56.67	33.33	21.67	10.00	0	-11.66
4000	220.00	175.00	135.00	93.33	35.00	23.33	11.66	-1.67	-13.33
4500	335.00	270.00	205.00	140.00	61.67	40.00	18.33	-3.33	-23.33
5000	550.00	440.00	330.00	226.67	118.33	75.00	33.33	-8.33	-48.33
5200	Failure.								

Table 5.1

CALCULATIONS OF EXPERIMENTAL AND COMPUTER M_x, ϕ_x, M_y, ϕ_y - COLUMN #1.

Experiment							Computer				
Load (kips)	M_x (kip in)	kd (inch)	ϕ_x 1/inch x 10^{-5}	M_y (kip in)	kd (inch)	ϕ_y 1/inch x 10^{-5}	Load (kips)	M_x (kip in)	ϕ_x 1/inch x 10^{-5}	M_y (kip in)	ϕ_y 1/inch x 10^{-5}
0	0	-	0	0	-	0	0	0	0	0	0
10.31	26.00	11.0	1.40	38.45	9.30	0.25	39.58	100.80	8.40	149.04	2.00
20.63	52.30	10.9	2.50	77.13	9.30	0.62	49.47	126.00	10.80	186.30	2.60
30.95	78.98	10.8	4.40	116.27	9.20	1.31	59.01	151.20	13.40	223.56	3.20
41.26	105.73	10.7	4.90	154.99	9.00	1.60	68.58	176.40	16.50	260.32	4.00
51.58	133.03	10.6	7.60	194.04	8.90	2.12	77.95	201.60	21.00	298.08	5.10
61.89	160.94	10.6	10.30	233.25	8.80	2.35	86.97	226.80	27.70	335.34	6.90
72.21	191.43	10.5	12.50	272.65	8.80	3.80	93.80	252.00	53.10	372.60	12.10
82.52	221.65	10.4	21.20	312.45	8.70	4.10	93.75	252.13	53.90	372.79	12.30
92.84	261.99	10.3	32.60	353.58	8.60	7.10	93.70	252.25	54.90	372.97	12.40
103.15	301.40	10.23	54.0	394.43	8.50	13.90		Failure			
107.28	Failure										

Table 5.2

CALCULATIONS OF EXPERIMENTAL AND COMPUTER M_x, ϕ_x, M_y, ϕ_y - COLUMN #2.

Experiment							Computer				
Load (kips)	M_x (kip in)	kd (inch)	ϕ_x 1/inch x 10^{-5}	M_y (kip in.)	kd (in.)	ϕ_y 1/inch x 10^{-5}	Load (kips)	M_x (kip in.)	ϕ_x 1/inch x 10^{-5}	M_y (kip in.)	ϕ_y 1/inch x 10^{-5}
0	0	-	0	0	-	0	0	0	0	0	0
10.31	29.00	10.9	1.00	42.76	9.1	0.40	49.24	140.20	12.30	207.00	3.0
20.63	58.22	10.8	3.00	85.49	9.1	0.80	58.87	168.24	15.40	248.40	3.7
30.95	87.65	10.8	5.00	128.29	9.0	1.30	68.31	196.28	19.70	289.80	4.8
41.26	118.21	10.7	7.00	172.10	8.9	2.00	77.49	224.32	25.80	331.20	6.4
51.58	148.55	10.5	11.00	215.66	8.9	2.20	85.64	252.36	40.50	372.60	9.9
61.89	180.29	10.4	14.00	259.13	8.7	2.40	85.98	253.76	41.90	374.67	10.2
72.21	212.15	10.2	20.00	303.57	8.6	4.50	86.30	255.17	43.40	376.74	10.6
82.52	246.65	10.2	24.50	348.32	8.6	7.20		Failure			
92.84	282.51	10.1	45.00	393.08	8.5	11.90					
97.99	Failure										

Table 5.3

CALCULATIONS OF EXPERIMENTAL AND COMPUTER M_x, ϕ_x, M_y, ϕ_y - COLUMN #3.

Experiment							Computer				
Load (kips)	M_x (kip in)	kd (inch)	ϕ_x 1/inch x 10^{-5}	M_y (kip in.)	kd (in.)	ϕ_y 1/inch x10^{-5}	Load (kips)	M_x (kip in.)	ϕ_x 1/inch x 10^{-5}	M_y (kip in.)	ϕ_y 1/inch x10^{-5}
0	0	-	0	0	-	0	0	0	0	0	0
10.31	31.91	10.7	1.2	46.97	8.8	0.40	19.87	61.70	5.9	91.08	1.4
20.63	64.16	10.6	2.5	94.11	8.7	0.90	29.68	92.56	9.3	136.62	2.2
30.95	96.66	10.5	7.0	141.26	8.5	1.80	39.42	123.41	12.8	182.15	3.1
41.26	129.56	10.3	12.0	188.68	8.4	2.90	49.05	154.26	17.0	227.70	4.1
51.58	163.77	10.2	15.0	236.13	8.3	4.00	58.42	185.11	23.6	273.24	5.8
61.89	197.61	10.1	23.5	284.08	8.3	5.00	67.09	215.97	38.0	318.78	9.2
72.21	239.02	10.0	38.0	333.90	8.2	9.90	67.47	217.51	39.3	321.06	9.5
74.27	Failure							Failure			

Table 5.4

CALCULATIONS OF EXPERIMENTAL AND COMPUTER M_x, ϕ_x, M_y, ϕ_y - COLUMN #4.

Experiment							Computer				
Load (kips)	M_x (kip in)	kd (inch)	ϕ_x 1/inch x 10^{-5}	M_y (kip in.)	kd (in.)	ϕ_y 1/inch x 10^{-5}	Load (kips)	M_x (kip in.)	ϕ_x 1/inch x 10^{-5}	M_y (kip in)	ϕ_y 1/in. x10^{-5}
0	0	-	0	0	-	0	0	0	0	0	0
10.31	34.80	10.3	2.6	51.33	8.3	0.60	29.66	101.13	10.3	149.07	2.5
20.63	69.74	10.2	7.0	102.90	8.2	1.63	39.39	134.84	14.2	198.76	3.4
30.95	104.88	10.2	9.9	154.50	8.2	2.12	48.97	168.54	19.5	248.45	4.7
41.26	140.19	10.0	13.5	206.11	8.0	3.13	58.23	202.25	28.3	298.14	7.0
51.58	175.51	9.8	20.9	258.00	7.8	5.13	59.12	205.63	29.6	303.12	7.4
61.89	210.94	9.6	28.9	309.98	7.6	8.99	59.99	209.00	31.4	308.09	7.8
66.02	Failure							Failure			

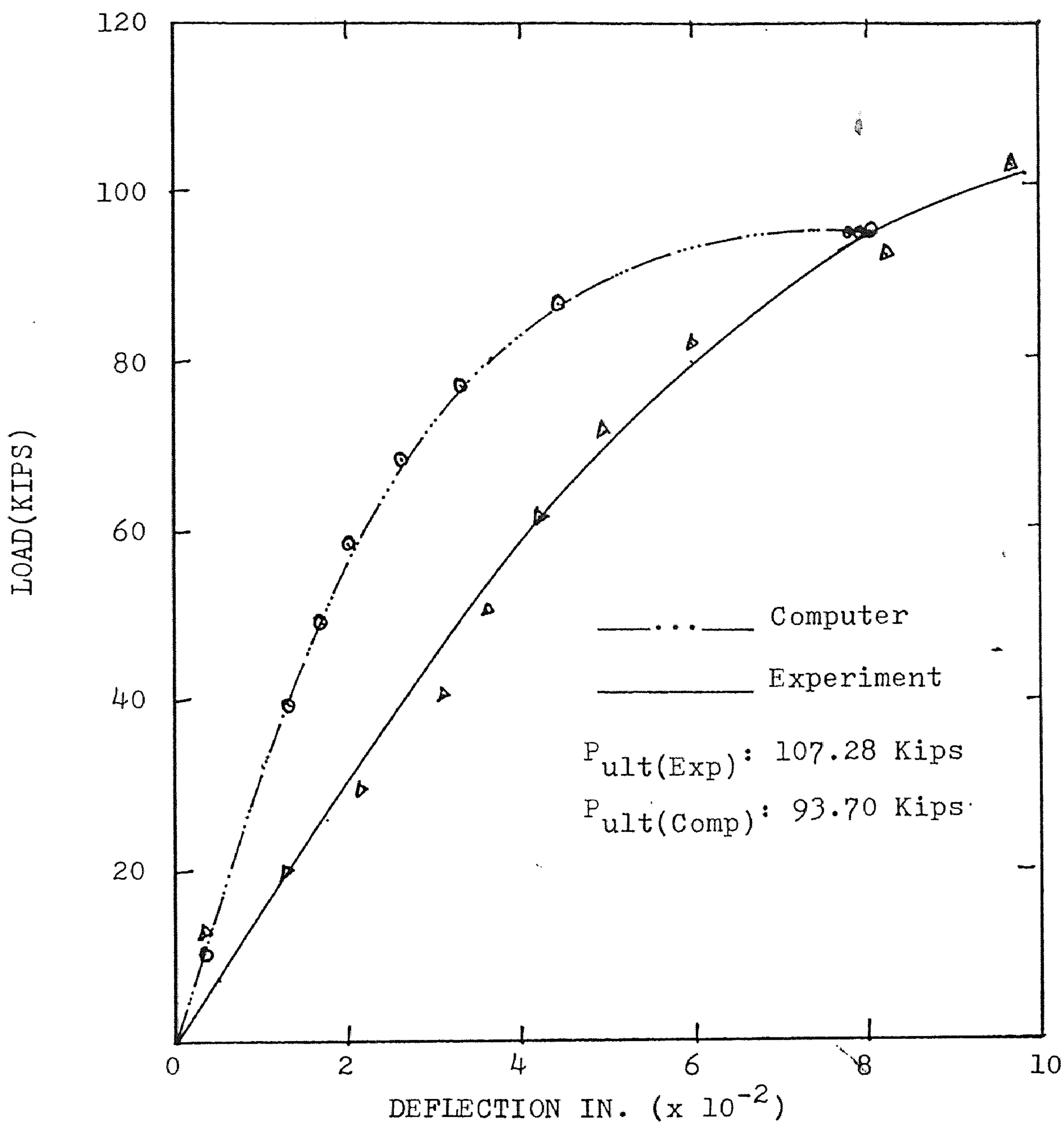

LOAD DEFLECTION CURVES IN
X-DIRECTION COLUMN #1.

Fig. 5.1.1

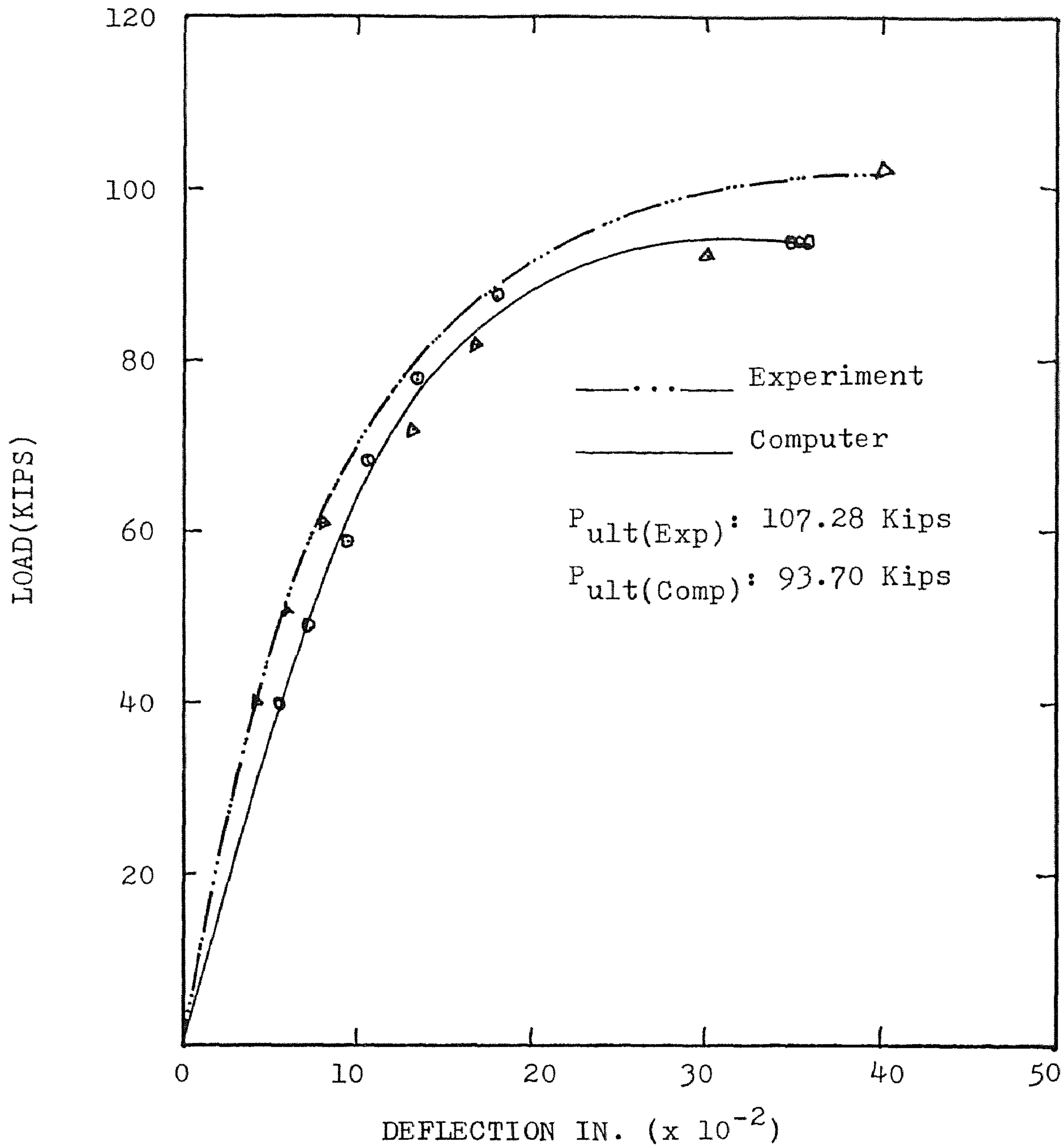

LOAD DEFLECTION CURVES IN
Y-DIRECTION COLUMN #1.

Fig. 5.1.2.

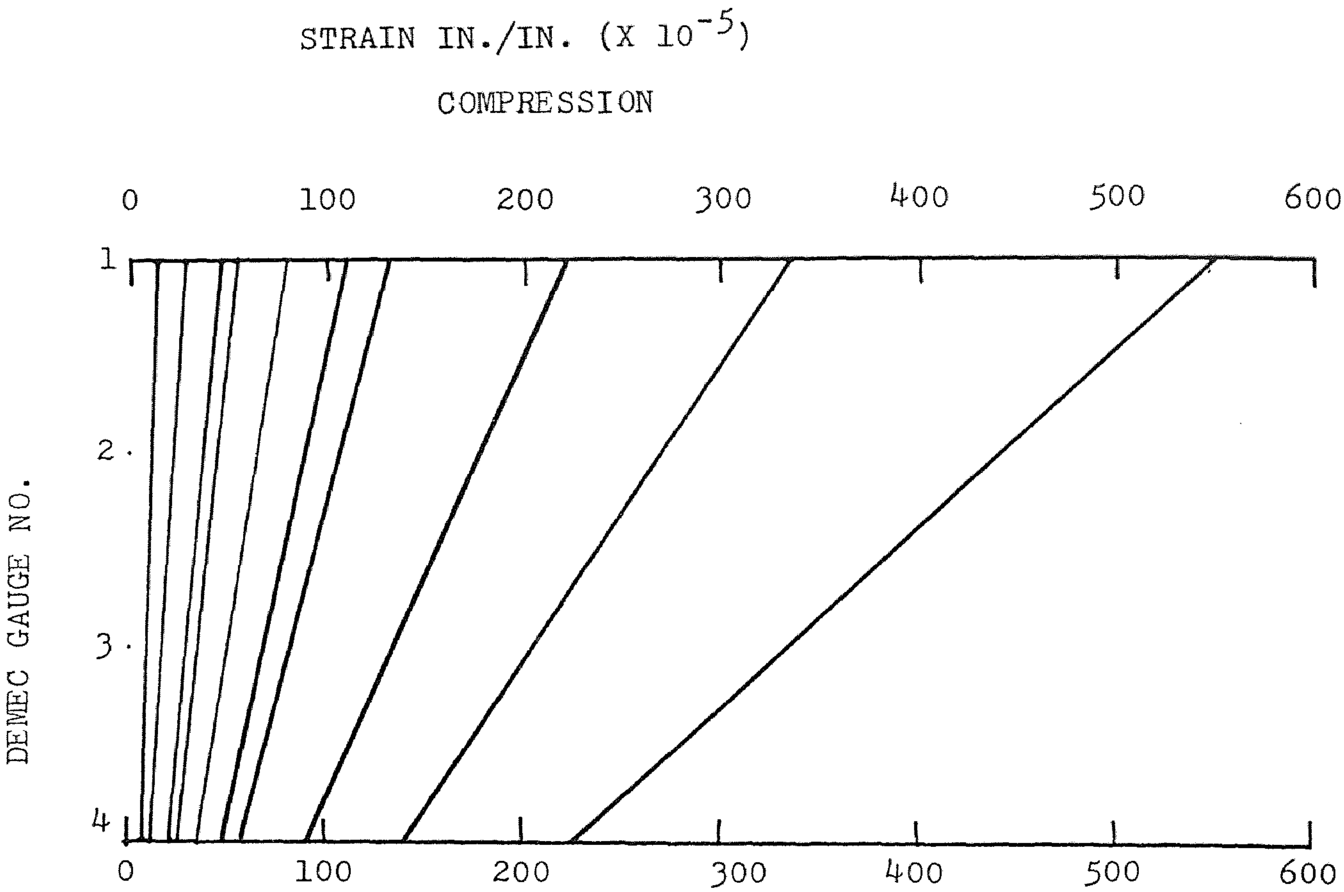

STRAIN DISTRIBUTION LEADING TO $\emptyset_X$

COLUMN #1.

Fig. 5.1.3

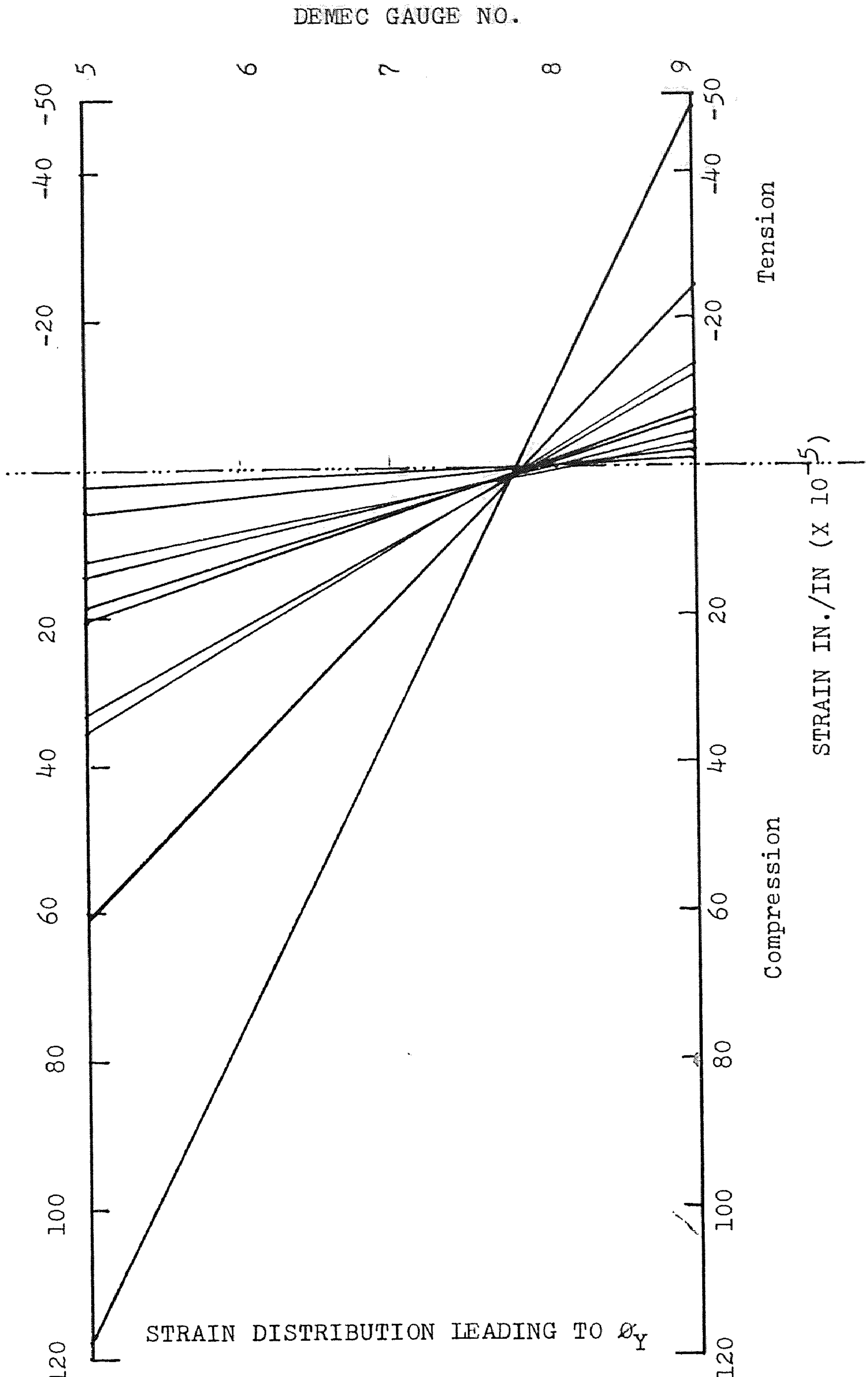

STRAIN DISTRIBUTION LEADING TO $\emptyset_Y$

COLUMN #1.

Fig. 5.1.4.

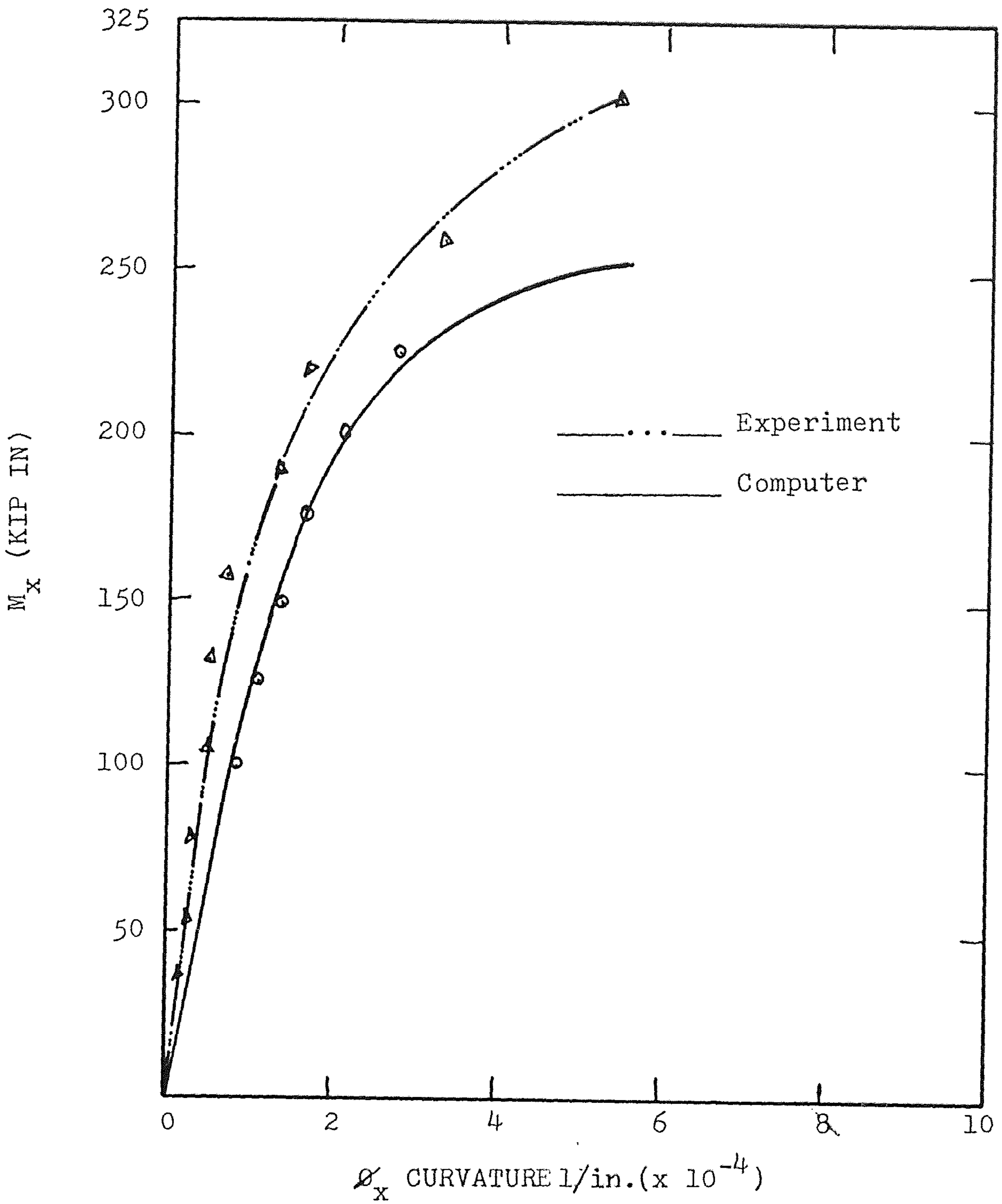

M_x - $\varnothing_x$ CURVE COLUMN #1.

Fig. 5.1.5.

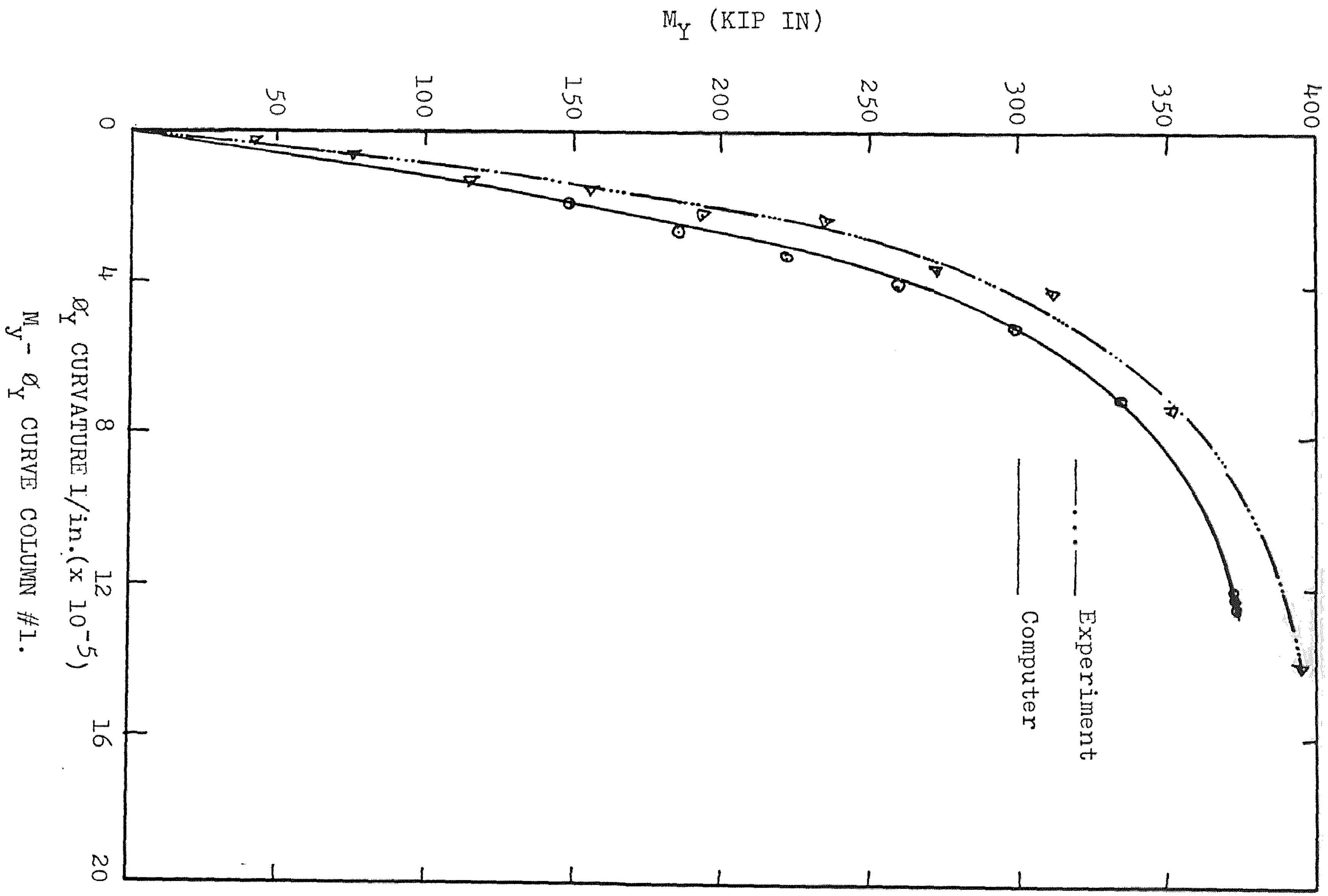
M_Y (KIP IN)
50
100
150
200
250
300
350
400
0
4
8
12
16
20
Experiment
Computer
ϕ_Y CURVATURE 1/in.(x 10^{-5})
M_Y - ϕ_Y CURVE COLUMN #1.

Fig. 5.1.6

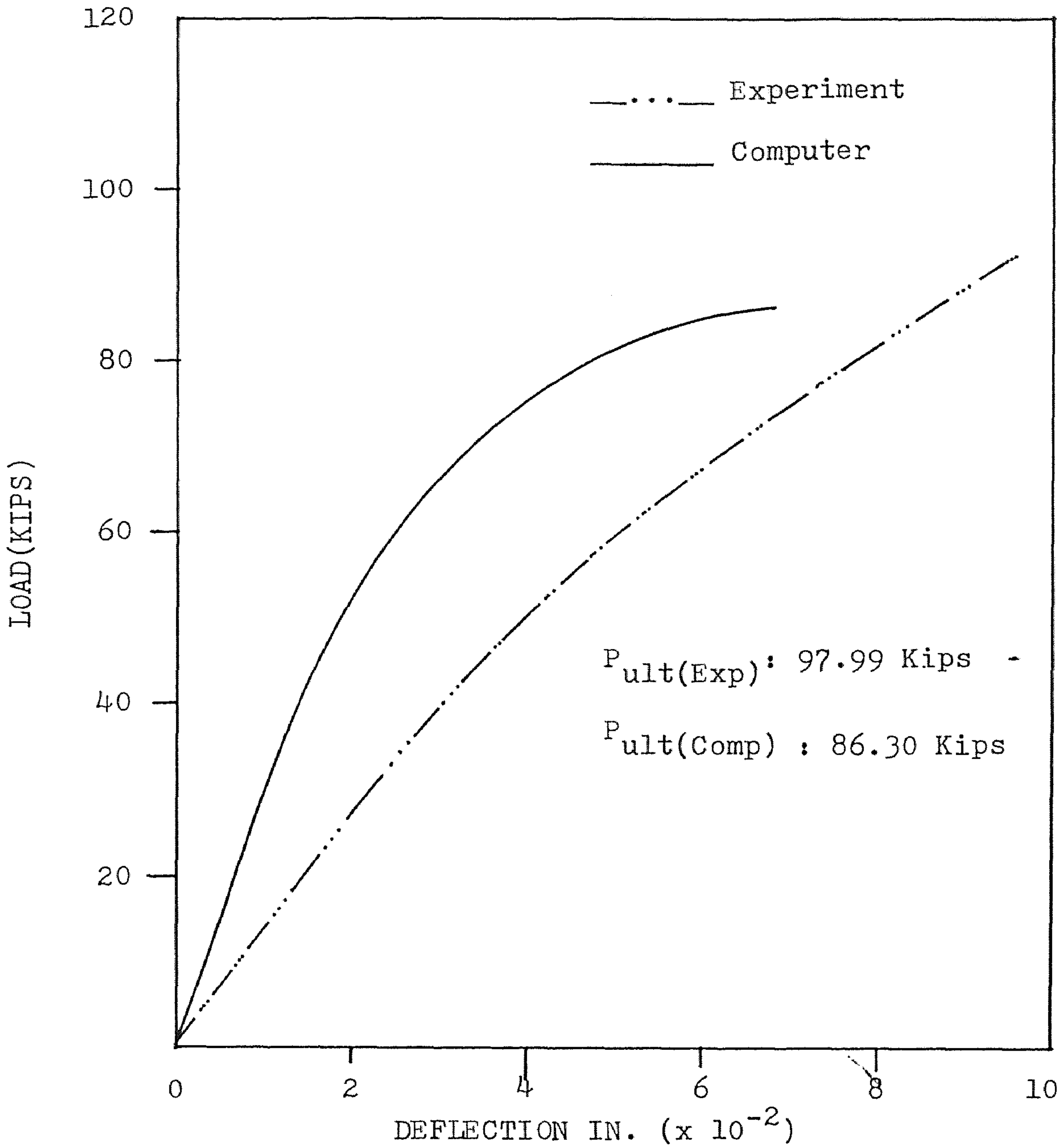

LOAD DEFLECTION CURVES IN
X-DIRECTION COLUMN #2.

Fig. 5.2.1

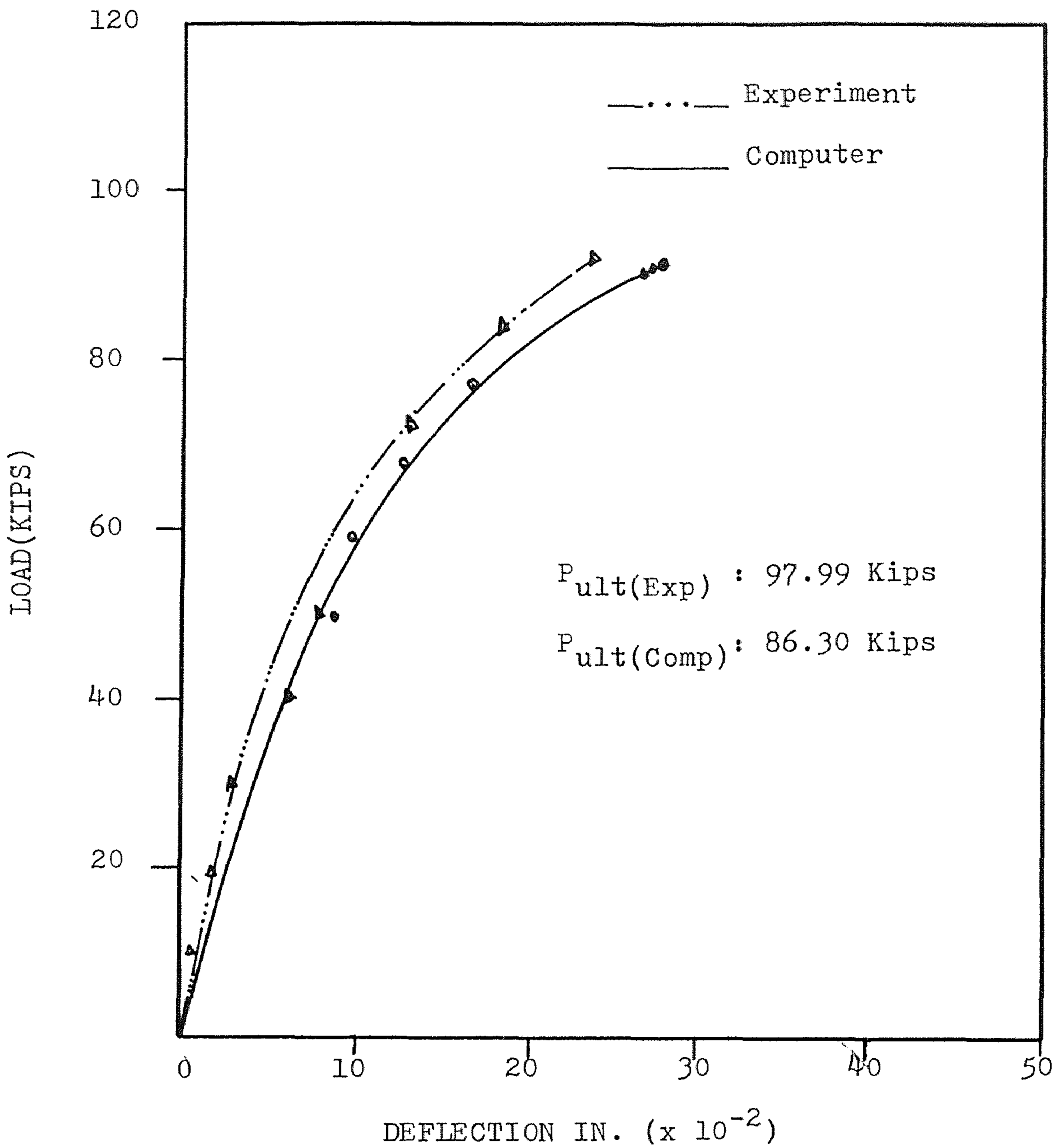

LOAD DEFLECTION CURVES IN
Y-DIRECTION COLUMN #2.

Fig. 5.2.2

STRAIN IN./IN. (X 10^{-5})
COMPRESSION

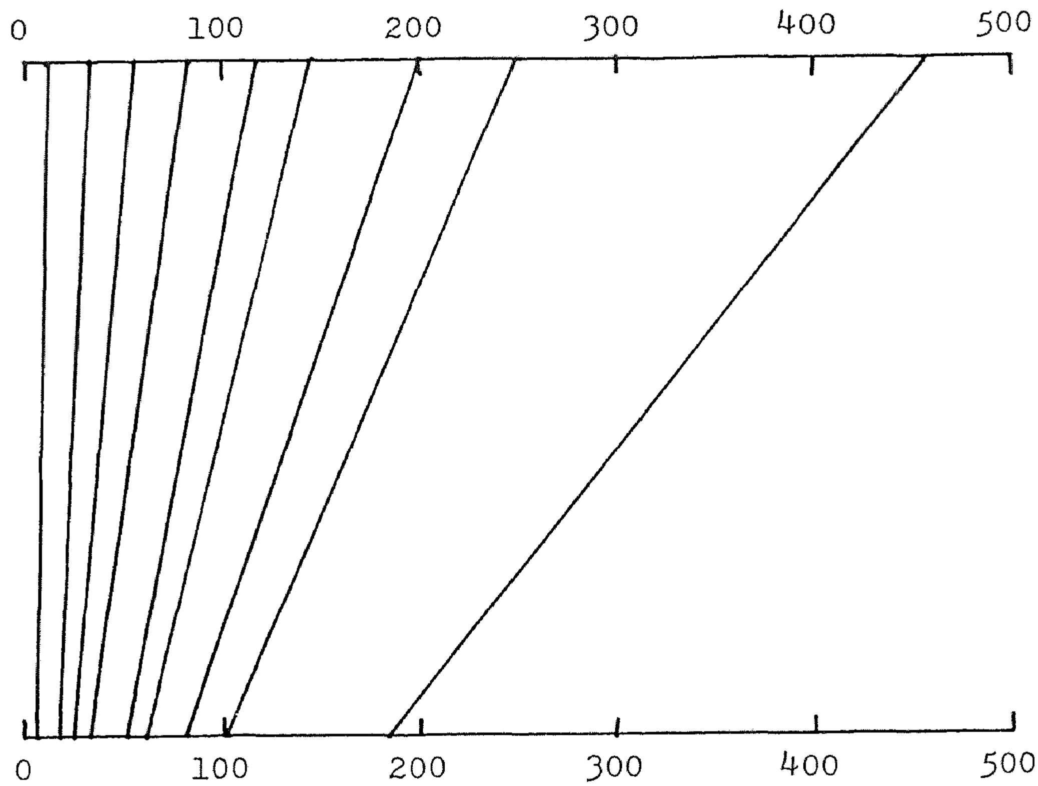

STRAIN DISTRIBUTION LEADING TO $\varnothing_X$
COLUMN #2.

Fig. 5.2.3

STRAIN DISTRIBUTION LEADING TO $Ø_Y$
COLUMN #2.

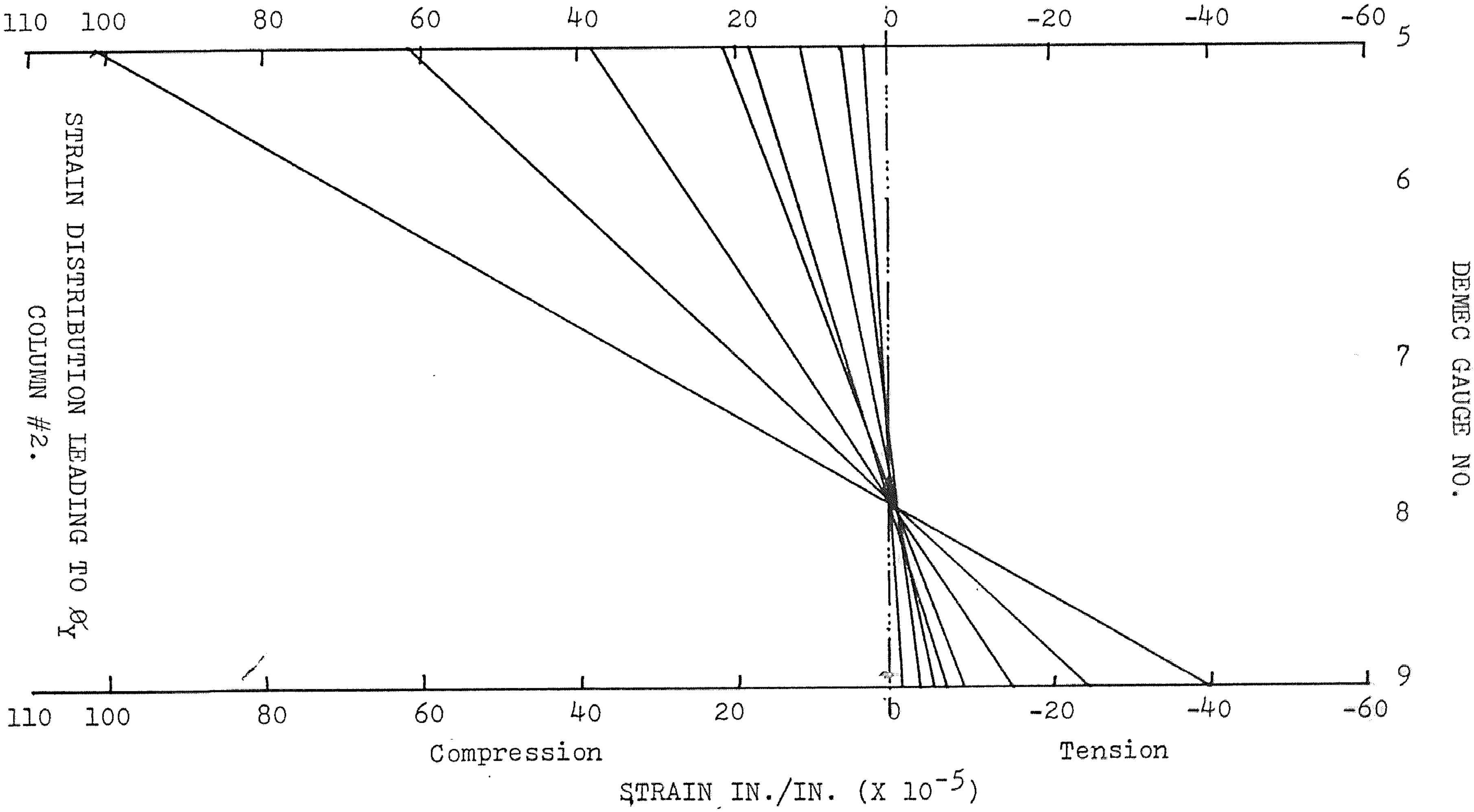

Fig. 5.2.4

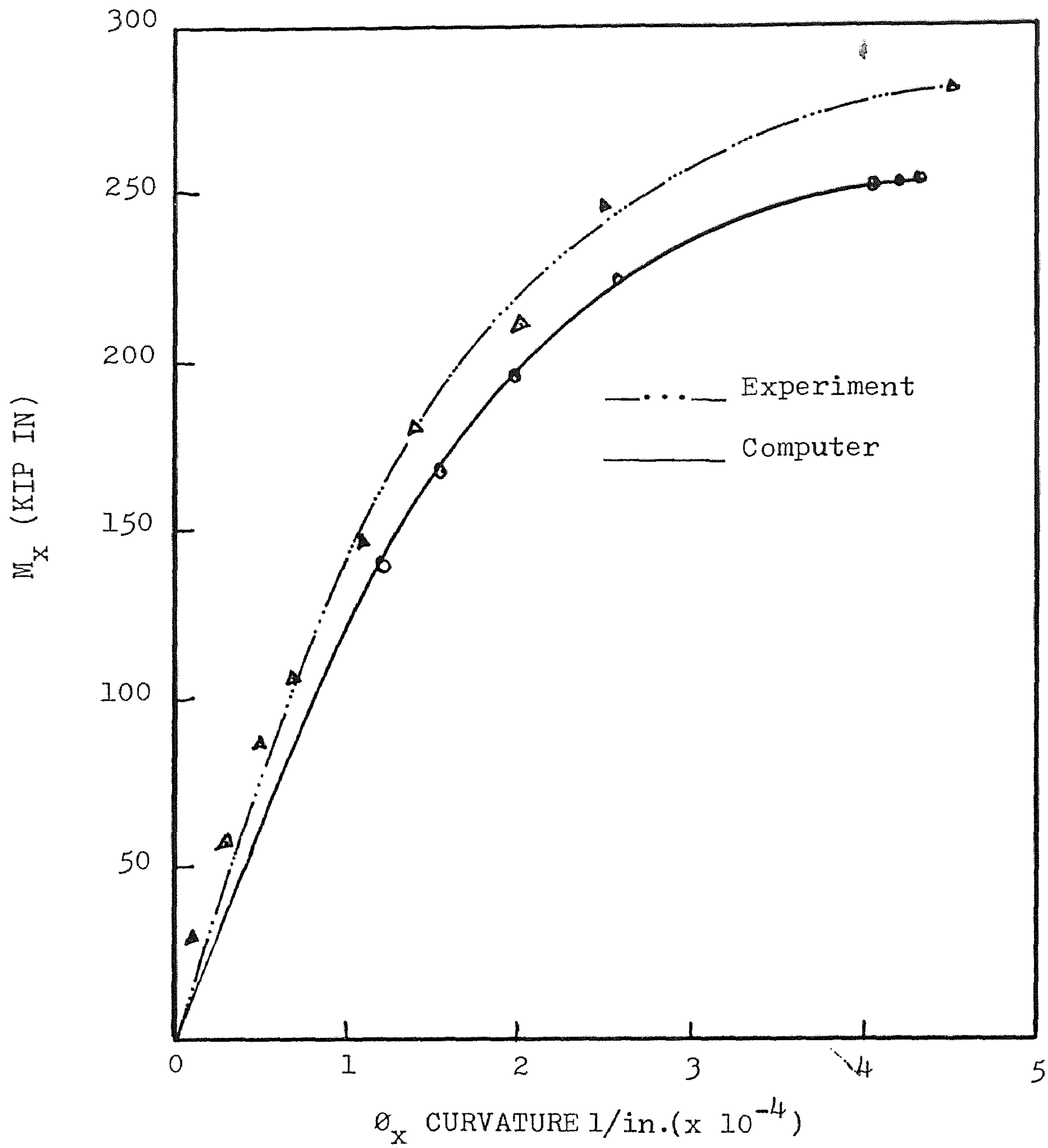

M_x - ϕ_x CURVE COLUMN #2

Fig. 5.2.5

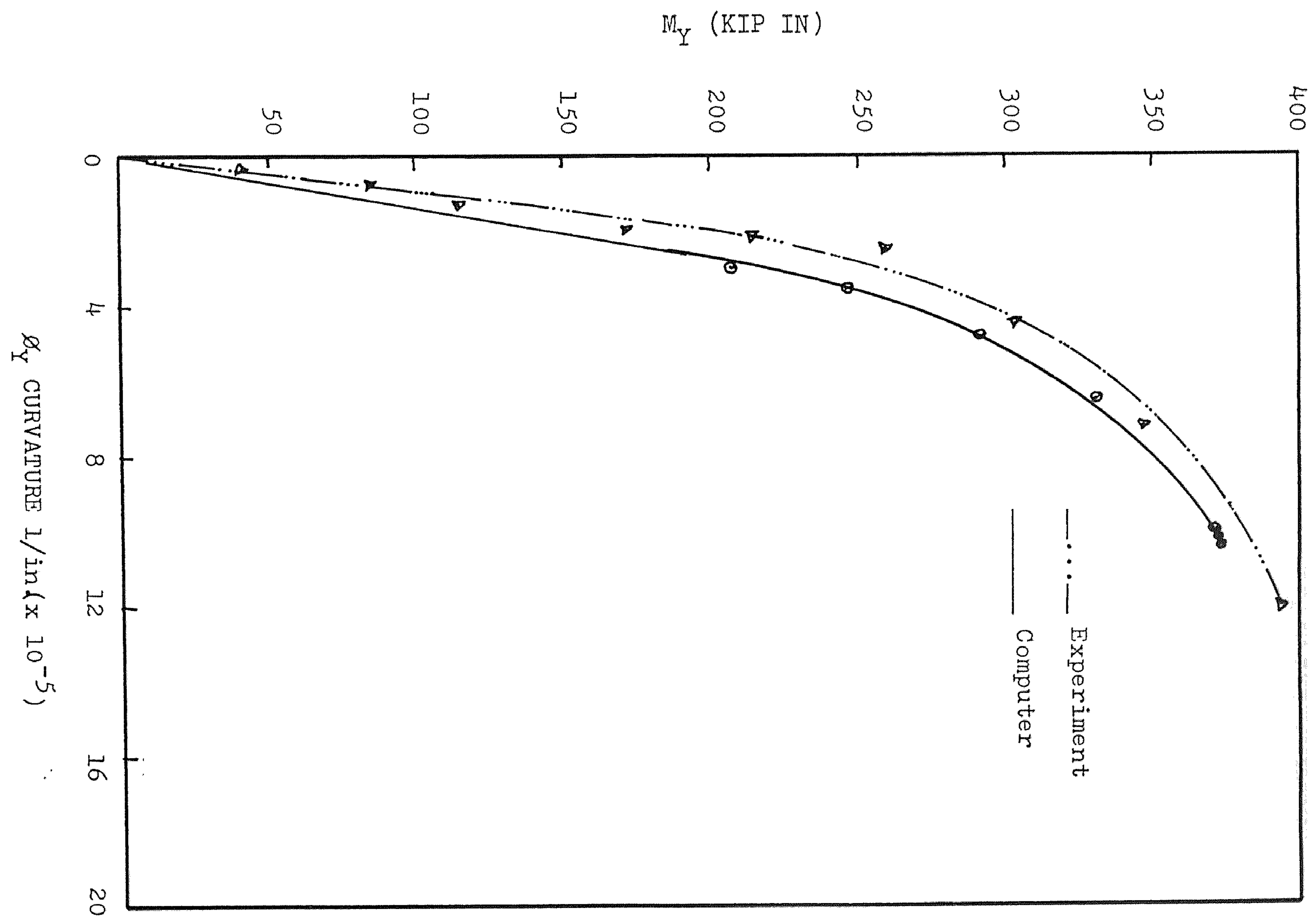

M_Y - $Ø_Y$ CURVE COLUMN #2.

Fig. 5.2.6

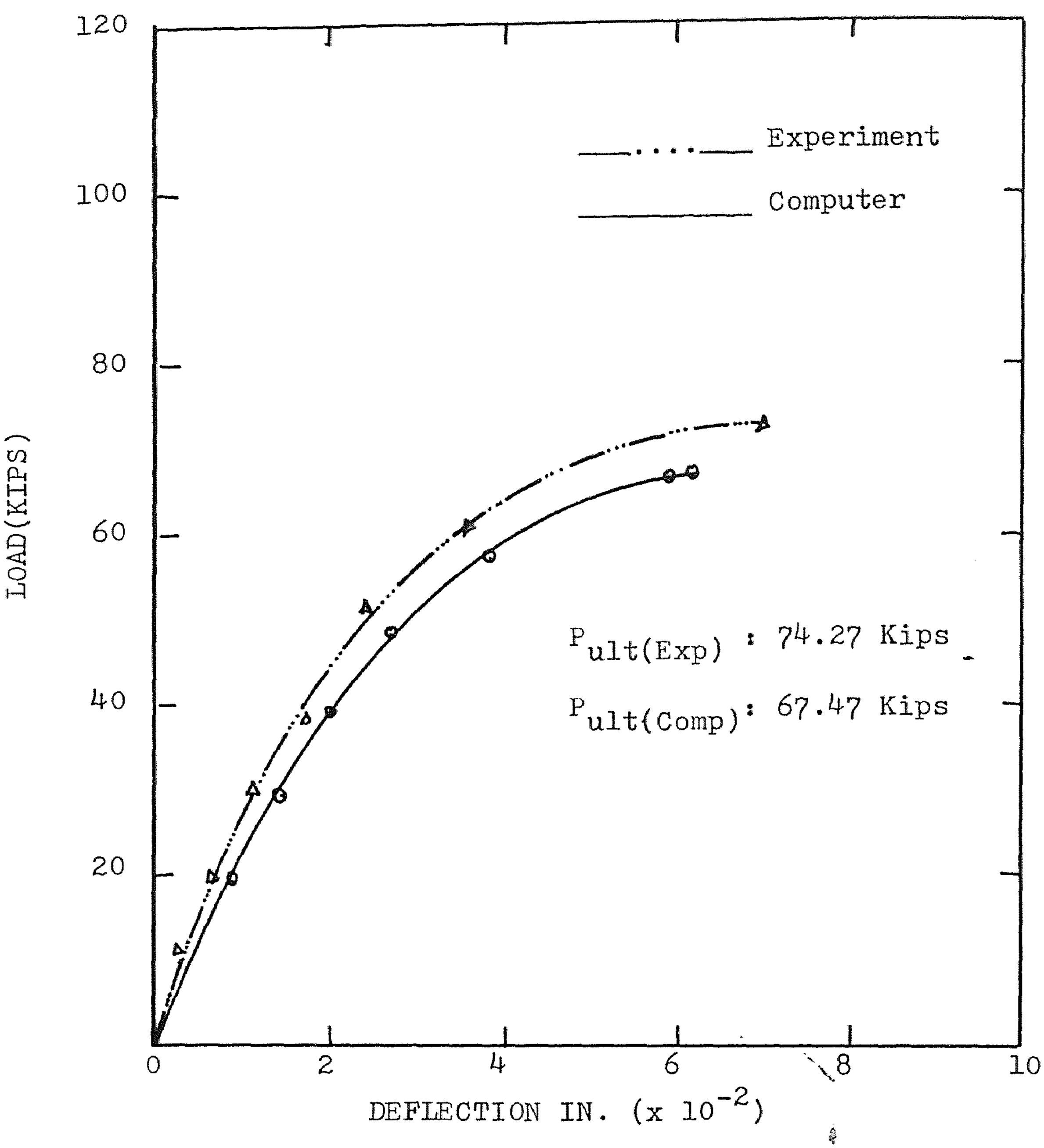

LOAD DEFLECTION CURVES IN
X-DIRECTION COLUMN #3.

Fig. 5.3.1

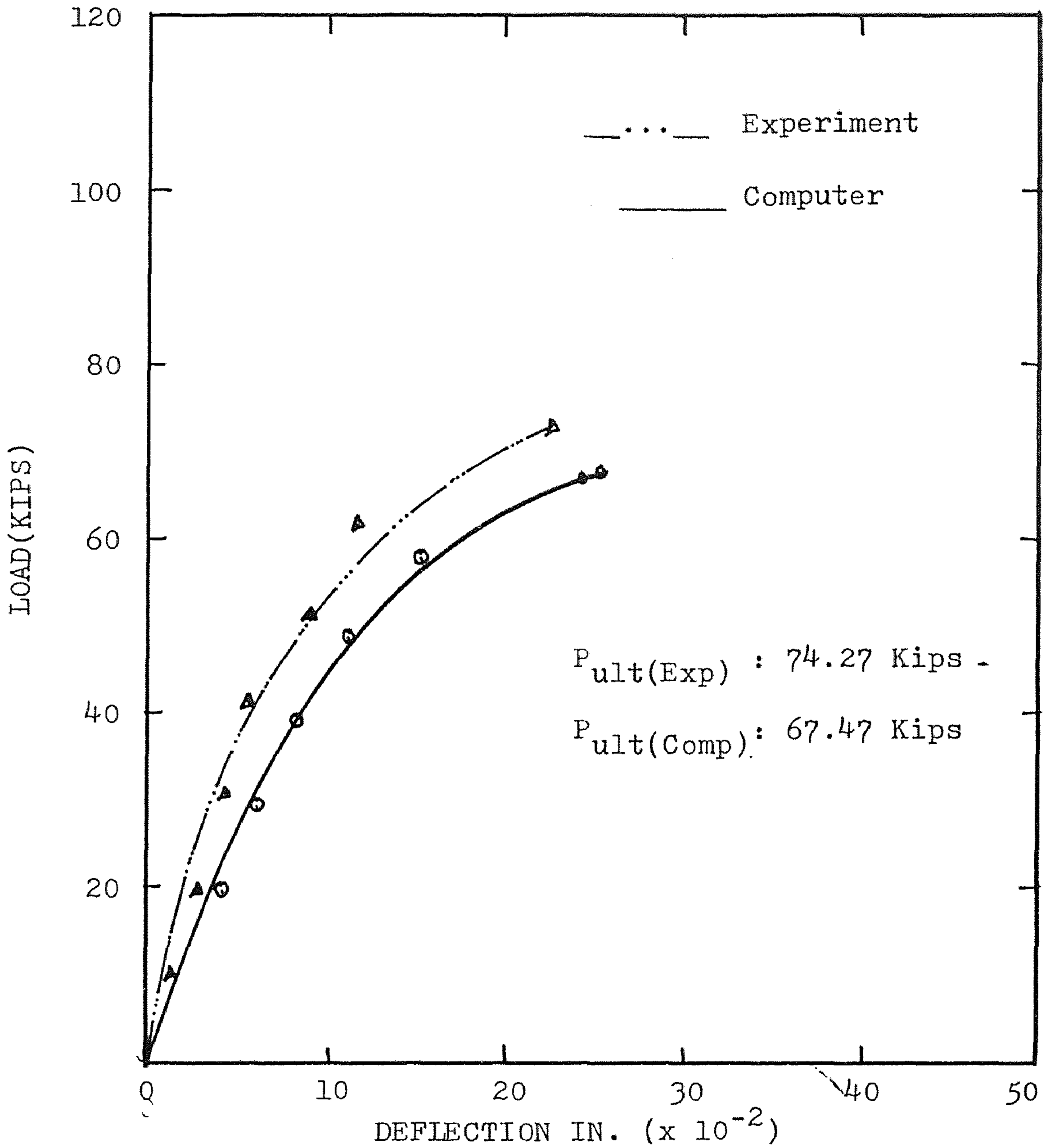

LOAD DEFLECTION CURVES IN
Y-DIRECTION COLUMN #3.

Fig. 5.3.2

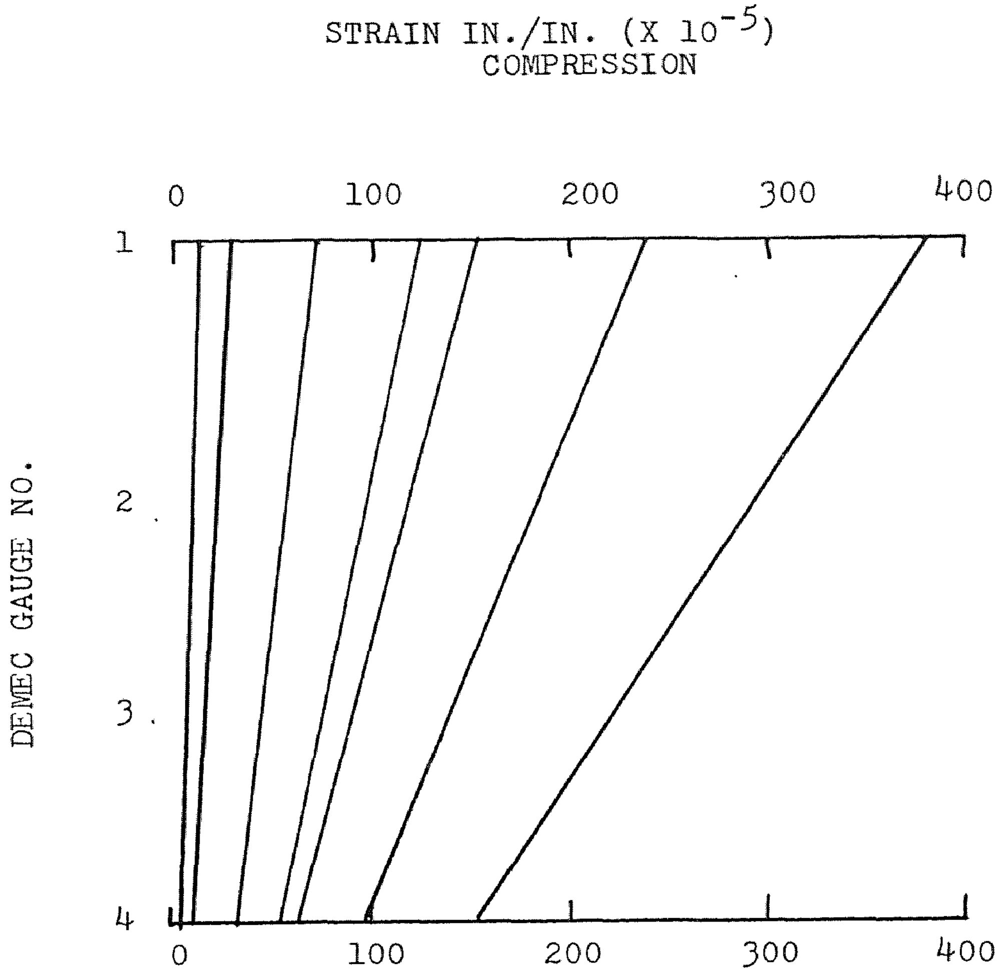

STRAIN DISTRIBUTION LEADING TO ϕ_X
COLUMN #3.

Fig. 5.3.3

STRAIN DISTRIBUTION LEADING TO $Ø_Y$
COLUMN #3.

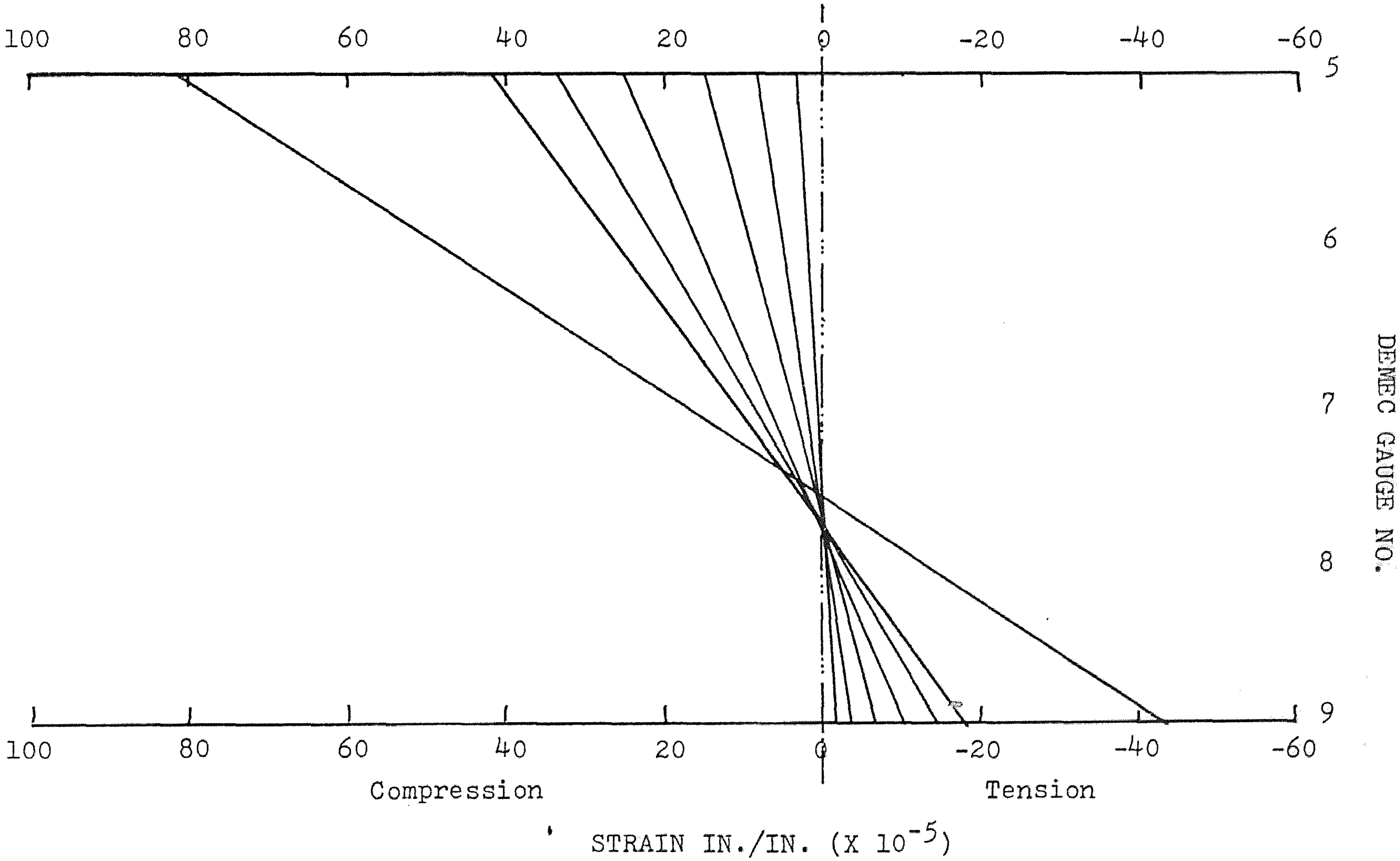

Fig. 5.3.4

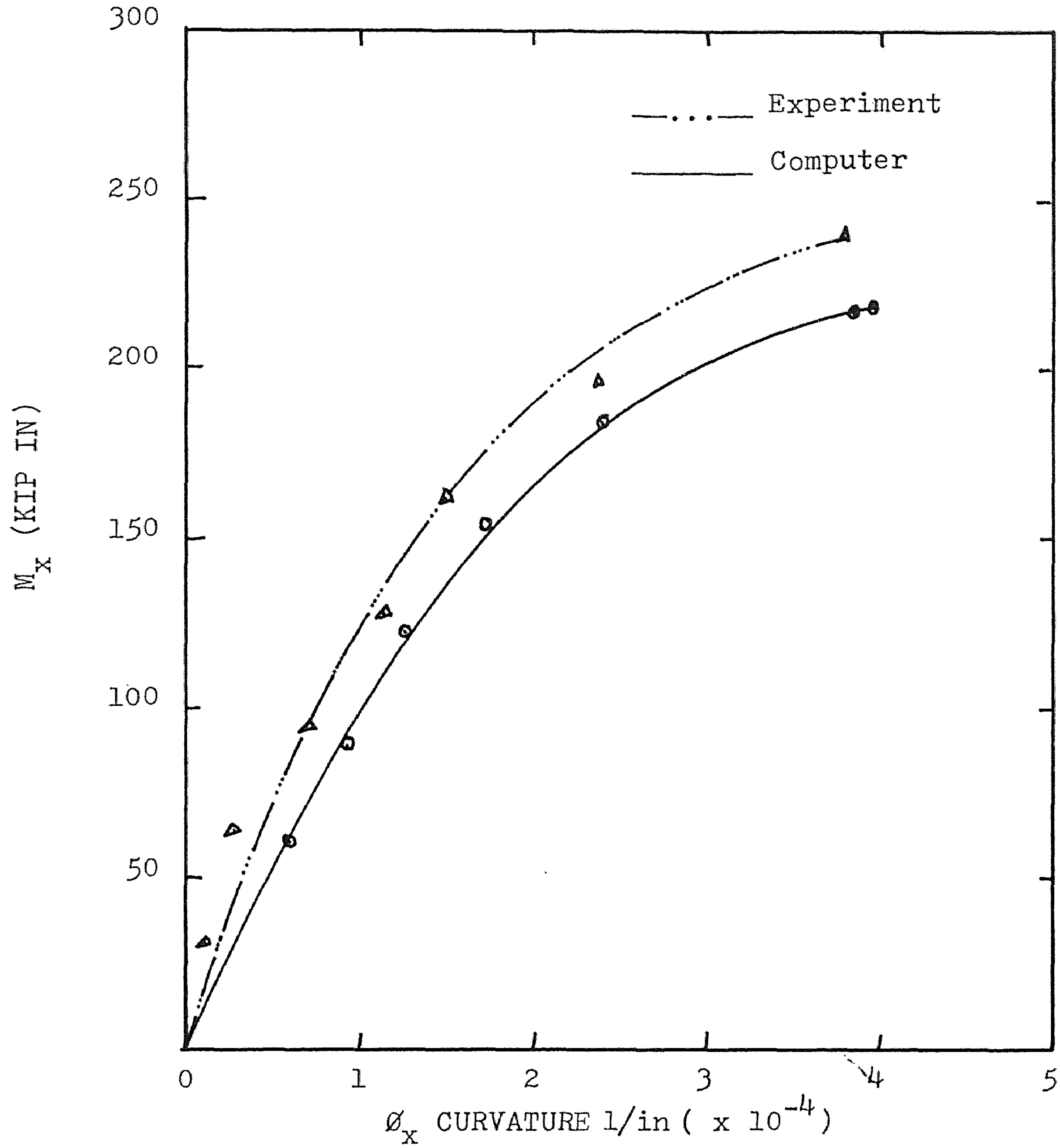

M_x - ϕ_x CURVE COLUMN #3.

Fig. 5.3.5

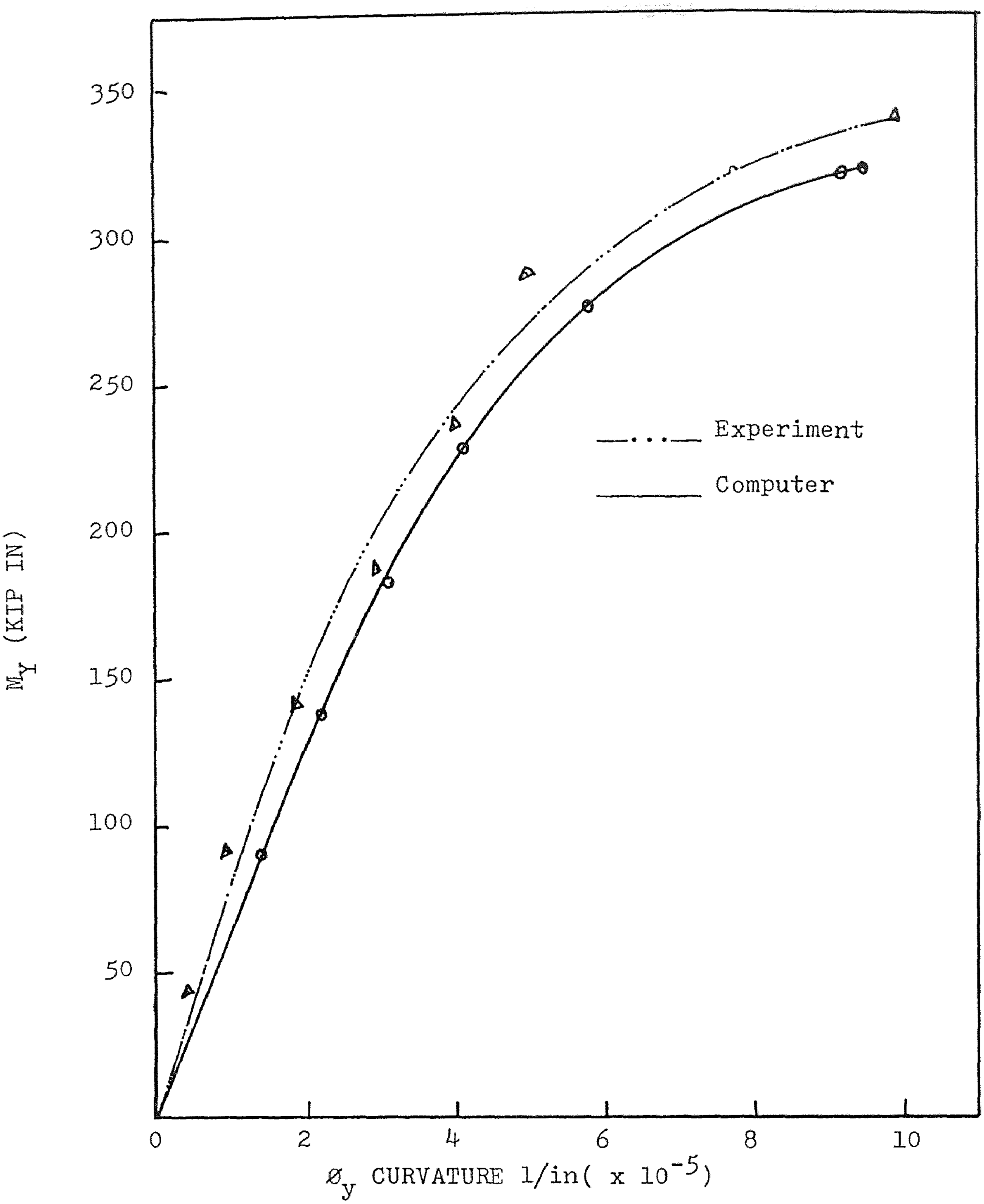

M_Y - $Ø_Y$ CURVE COLUMN #3

Fig. 5.3.6

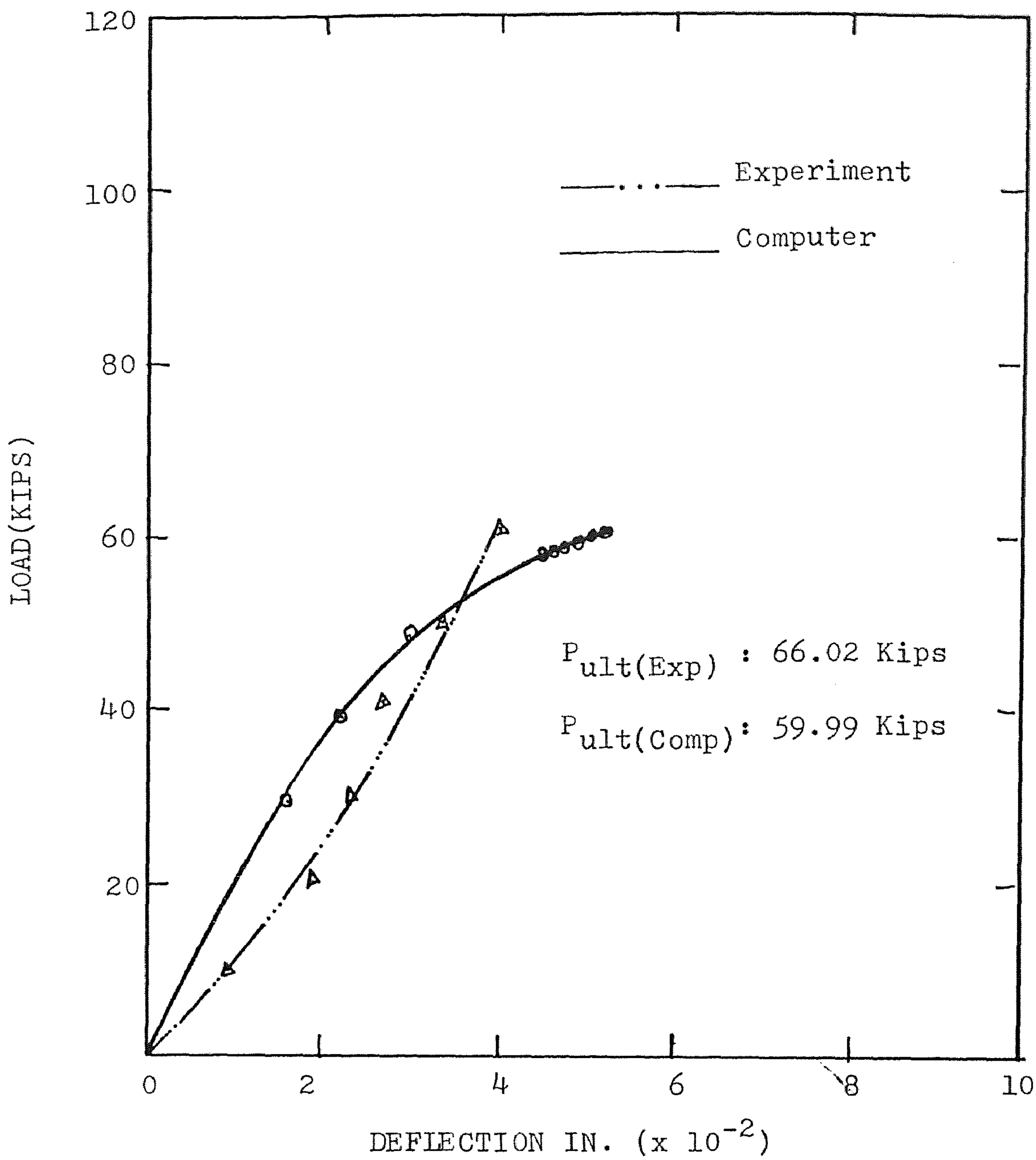

LOAD DEFLECTION CURVES IN
X-DIRECTION COLUMN #4.

Fig. 5.4.1

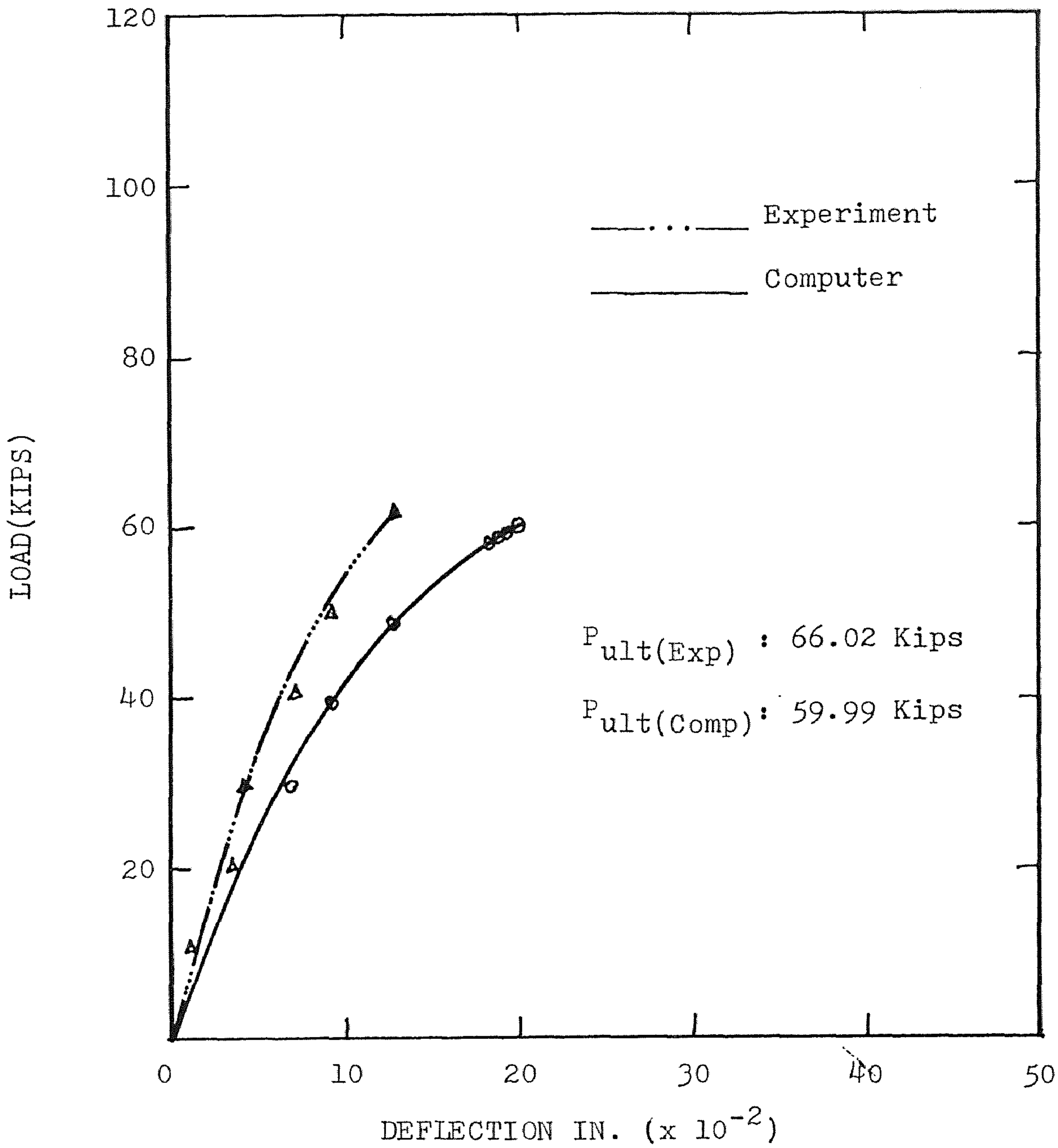

LOAD DEFLECTION CURVES IN
Y-DIRECTION COLUMN #4.

Fig. 5.4.2

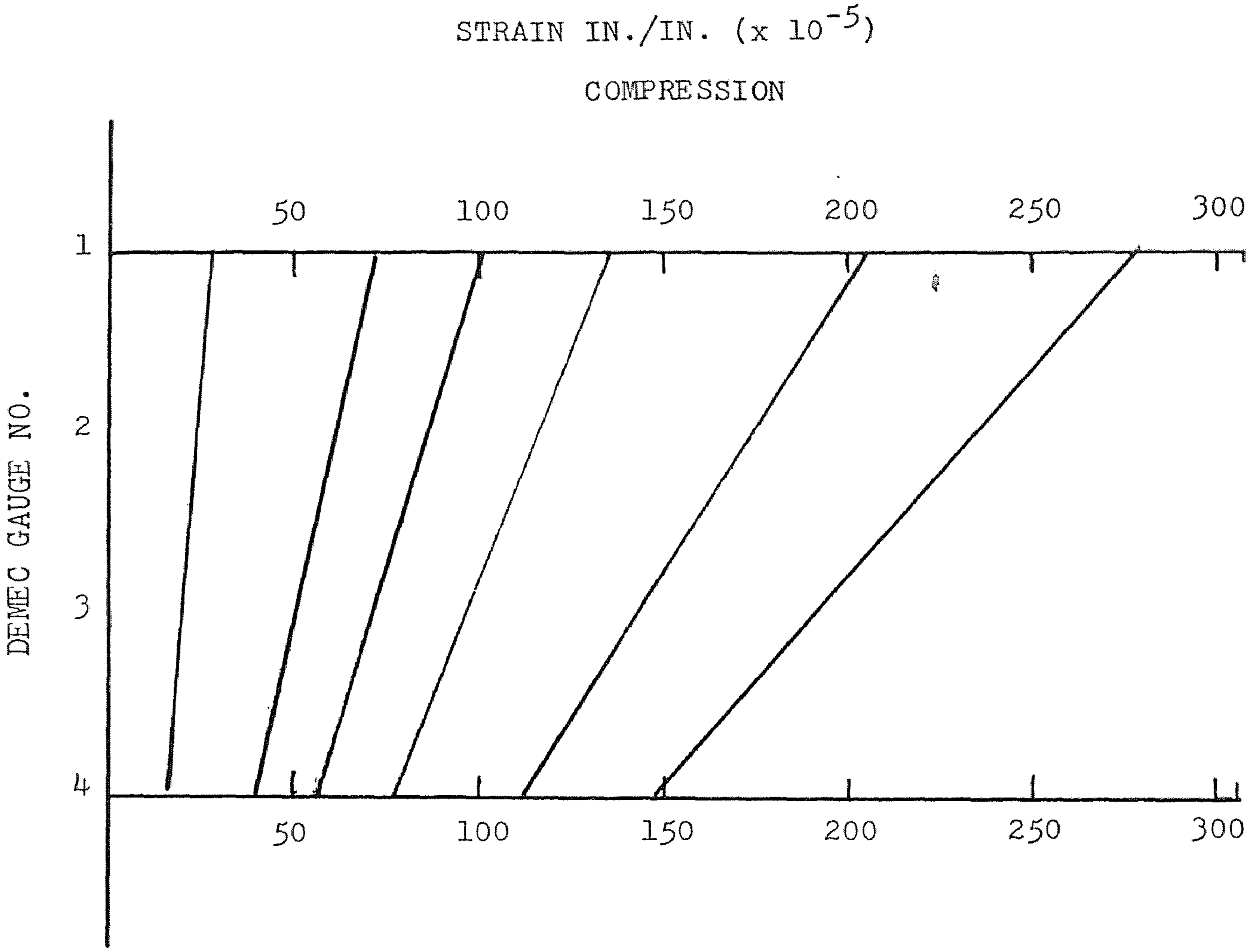

STRAIN DISTRIBUTION LEADING TO ϕ_X

COLUMN #4.

Fig. 5.4.3

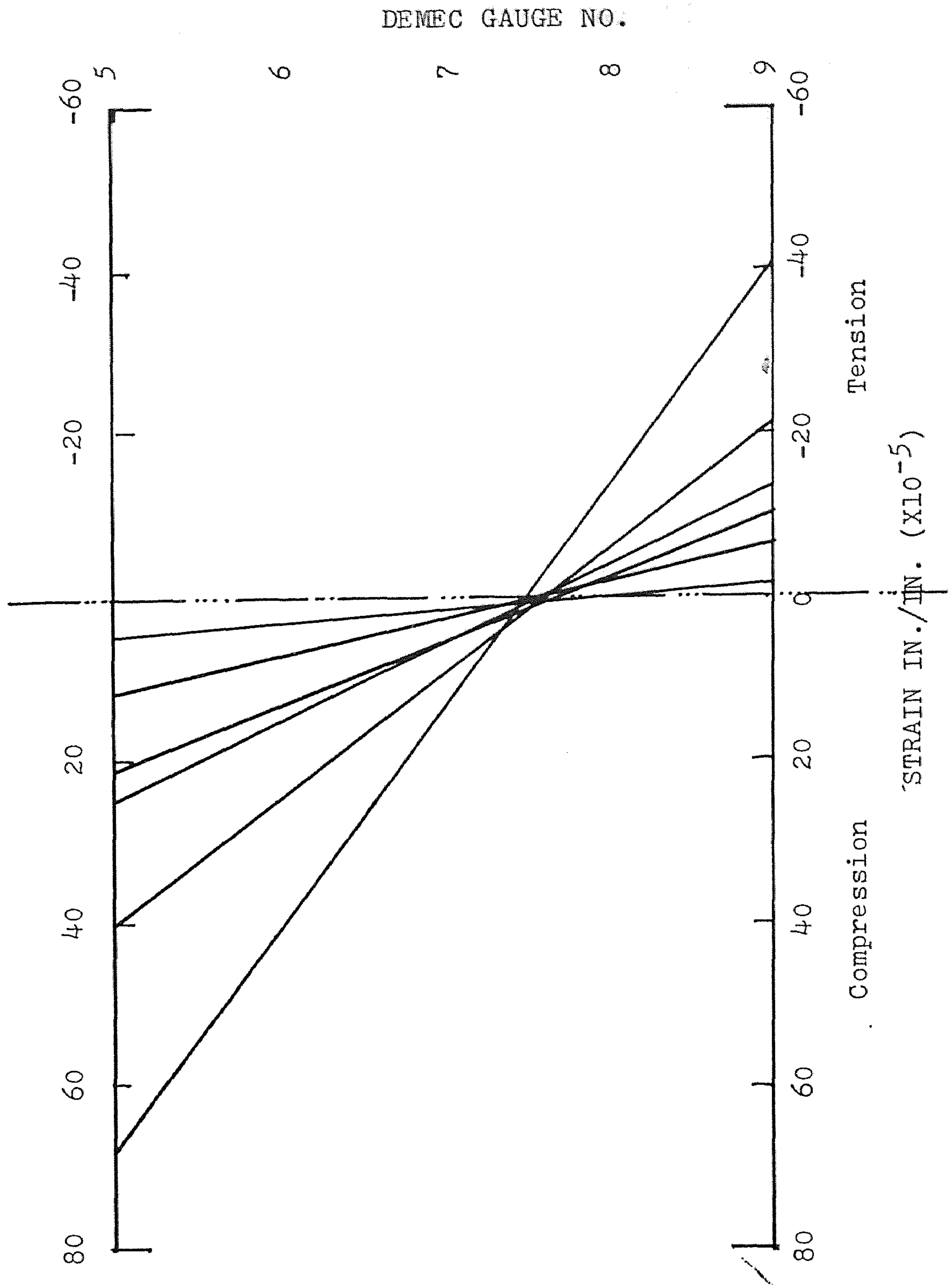

STRAIN DISTRIBUTION LEADING TO ϕ_Y

COLUMN #4.

Fig. 5.4.4

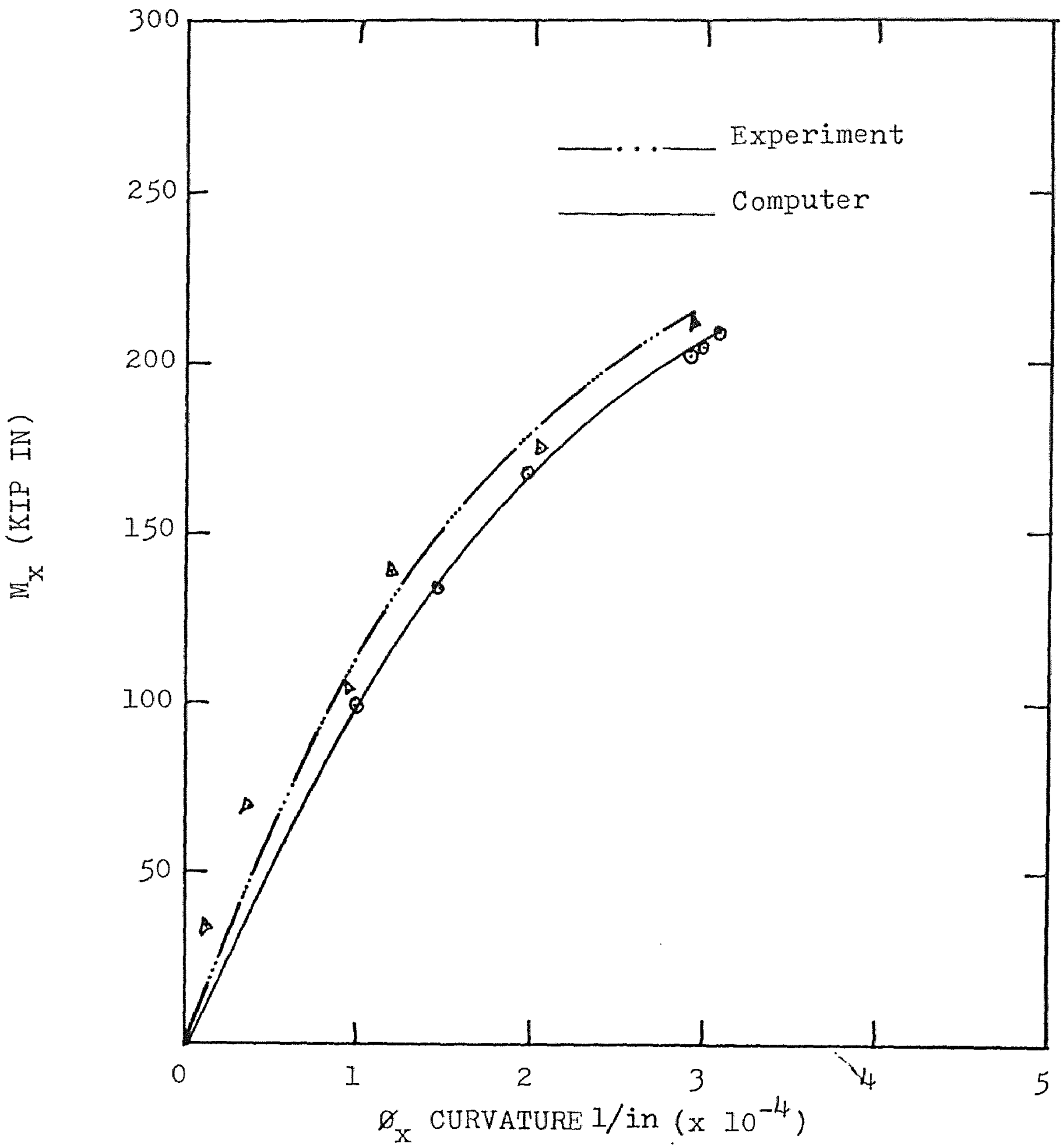

M_x - ϕ_x CURVE COLUMN #4.

Fig. 5.4.5

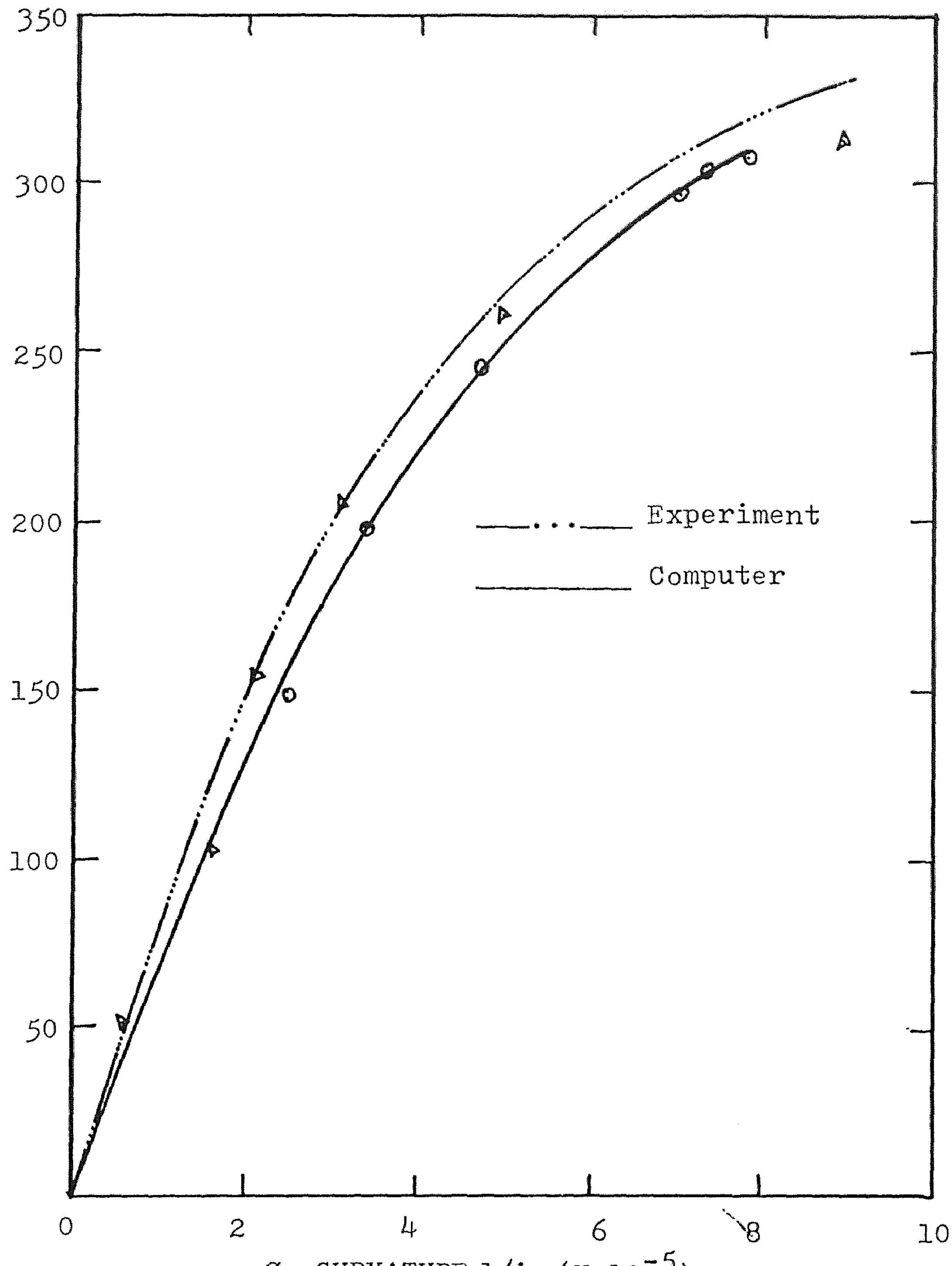

M_Y - ϕ_Y CURVE COLUMN #4.

Fig. 5.4.6

CHAPTER VI. CONCULUSION AND DISCUSSION OF RESULTS

1) Presently, both beam and column strength under the ACI Building Code is based on a limiting compressive concrete strain criterion of 0.003in/in. Application of this failure criterion of 0.003 in/in. to columns was based on tests of statically determinate columns which became unstable when the first hinge(maximum moment resistance) developed in the specimens. This criterion was adopted primarily because it represented a lower bound of the measured strains at maximum flexural resistance. However, due to the type of instrumentation which was used in many instances the concrete compressive strain at the exact point of maximum moment resistance or at the instant of the release of the members could not be determined. It is possible that higher compressive strains existed from the time the members became unstable until the energy release of the systems occured.

2)Compression crushing was observed over an extended zone. Large column strains and curvatures was observed before failure. The measured curvatures were also much larger than generally though possible for concrete columns with axial load and biaxial bending. The large magnitude of these observed strains and curvatures made interpretation of the test results difficult when using M-Ø relationships.

3) The experimental M-ϕ curves were plotted using the computed moments and the measured curvature at stations near the failure region. Theoretical curves based on results obtained from computer program developed by Hsu[1] were almost superimposed on the experimental curves for comparison. The theoretical M-ϕ curve obtained from computer results does not take into account moment gradient and was not based on data collected using the said type of instrumentation or loading technique. Consequently theoretical curve accurately predicts strength but does not reflect the deformation capacity shown by the experimental curves. Therefore the theoretical curves are much more accurate representation of the magnitude of deformation and are generally on the conservative side. This can be clearly observed from M-ϕ curves, i.e. the theoretical curves are well below the experimental curves indicating conservativeness.

4) The experimental strains shown were calculated assuming linear strain profiles from the demec gages and the strains recorded are average strains over 6 in. gage length. Approximate curvatures beyond maximum moment could be calculated because the gages on the tension side of the specimen were apparently broken by the development of a crack beneath them.

5) The relatively long, nearly flat-topped, latter

portion of the M-Ø relationships indicates that the highly loaded columns with high strength concrete and minimal ties can provide the capability for significant post yielding redistribution of moments in monotonically loaded concrete columns.

6) An extensive series of equilibrium checks was carried out to verify the measured moment values. Minor corrections were required to account for small movements of jacking piston and end plate and a few missing or disturbed instruments. Overall the maximum inaccuracy in measured moments is about 4 percent, which is well within acceptable limits.

7) Considerably greater ductility exists in lightly tied heavily loaded concrete columns than usually predicted by M-Ø relationships.

8) A few experimental load-deflection curves did not duplicate the analysis results, may be due to the experimental errors.

9) Although thin-walls in nature, the specimens subjected to biaxially eccentric loads were not failed by shear, rather all the specimens were characterized as compression failure.

10) In general an excellent agreement of experimental results was found with that of results obtained from computer program developed by Hsu[1].

APPENDIX 1.

Area and Coordinates of the elements of Channel Section.

Element	Area	X-Coordinate	Y-Coordinate
1	0.1100	-6.7500	4.3330
2	0.1100	-6.7500	2.8330
3	0.1100	-6.7500	1.3330
4	0.1100	-6.7500	-0.1670
5	0.1100	-6.7500	-1.6670
6	0.1100	-5.2500	-1.6670
7	0.1100	-3.7500	-1.6670
8	0.1100	-2.2500	-1.6670
9	0.1100	-0.7500	-1.6670
10	0.1100	0.7500	-1.6670
11	0.1100	2.2500	-1.6670
12	0.1100	3.7500	-1.6670
13	0.1100	5.2500	-1.6670
14	0.1100	6.7500	-1.6670
15	0.1100	6.7500	-0.1670
16	0.1100	6.7500	1.3330
17	0.1100	6.7500	2.8330
18	0.1100	6.7500	4.3330
19	0.3160	-6.2810	4.8020
20	0.2110	-6.7500	4.8020
21	0.3160	-7.2190	4.8020
22	0.2110	-7.2190	4.3330

Element	Area	X-Coordinate	Y-Coordinate
23	0.3160	-7.2190	3.8640
24	0.3160	-7.2190	3.3020
25	0.2110	-7.2190	2.8330
26	0.3160	-7.2190	2.3640
27	0.3160	-7.2190	1.8020
28	0.2110	-7.2190	1.3330
29	0.3160	-7.2190	0.8640
30	0.3160	-7.2190	0.3020
31	0.2110	-7.2190	-0.1670
32	0.3160	-7.2190	-0.6360
33	0.3160	-7.2190	-1.1980
34	0.2110	-7.2190	-1.6670
35	0.3160	-7.2190	-2.1360
36	0.2110	-6.7500	-2.1360
37	0.3160	-6.2810	-2.1360
38	0.3160	-5.7190	-2.1360
39	0.2110	-5.2500	-2.1360
40	0.3110	-4.7810	-2.1360
41	0.3160	-4.2190	-2.1360
42	0.2110	-3.7500	-2.1360
43	0.3160	-3.2810	-2.1360
44	0.3160	-2.7190	-2.1360
45	0.2110	-2.2500	-2.1360
46	0.3160	-1.7810	-2.1360

Element	Area	X-Coordinate	Y-Coordinate
47	0.3160	-1.2190	-2.1360
48	0.2110	-0.7500	-2.1360
49	0.3160	-0.2810	-2.1360
50	0.3160	0.2180	-2.1360
51	0.2110	0.7500	-2.1360
52	0.3160	1.2190	-2.1360
53	0.3160	1.7810	-2.1360
54	0.2110	2.2500	-2.1360
55	0.3160	2.7190	-2.1360
56	0.3160	3.2810	-2.1360
57	0.2110	3.7500	-2.1360
58	0.3160	4.2190	-2.1360
59	0.3160	4.7810	-2.1360
60	0.2110	5.2500	-2.1360
61	0.3160	5.7190	-2.1360
62	0.3160	6.2810	-2.1360
63	0.2110	6.7500	-2.1360
64	0.3160	7.2190	-2.1360
65	0.2110	7.2190	-1.6670
66	0.3160	7.2190	-1.1980
67	0.3160	7.2190	-0.6360
68	0.2110	7.2190	-0.1670
69	0.3160	7.2190	0.3020
70	0.3160	7.2190	0.8640

Element	Area	X-Coordinate	Y-Coordinate
71	0.2110	7.2190	1.3330
72	0.3160	7.2190	1.8020
73	0.3160	7.2190	2.3640
74	0.2110	7.2190	2.8330
75	0.3160	7.2190	3.3020
76	0.3160	7.2190	3.8640
77	0.2110	7.2190	4.3330
78	0.3160	7.2190	4.8020
79	0.2110	6.7500	4.8020
80	0.3160	6.2810	4.8020
81	0.2110	6.2810	4.3330
82	0.3160	6.2810	3.8640
83	0.3160	6.2810	3.3020
84	0.2110	6.2810	2.8330
85	0.3160	6.2810	2.3640
86	0.3160	6.2810	1.8020
87	0.2110	6.2810	1.3330
88	0.3160	6.2810	0.8640
89	0.3160	6.2810	0.3020
90	0.2110	6.2810	-0.1670
91	0.3160	6.2810	-0.6360
92	0.3160	6.2810	-1.1980
93	0.3160	5.7190	-1.1980
94	0.2110	5.2500	-1.1980

Element	Area	X-Coordinate	Y-Coordinate
95	0.3160	4.7810	-1.1980
96	0.3160	4.2190	-1.1980
97	0.2110	3.7500	-1.1980
98	0.3160	3.2810	-1.1980
99	0.3160	2.7190	-1.1980
100	0.2110	2.2500	-1.1980
101	0.3160	1.7810	-1.1980
102	0.3160	1.2190	-1.1980
103	0.2110	0.7500	-1.1980
104	0.3160	0.2810	-1.1980
105	0.3160	-0.2810	-1.1980
106	0.2110	-0.7500	-1.1980
107	0.3160	-1.2190	-1.1980
108	0.3160	-1.7810	-1.1980
109	0.2110	-2.2500	-1.1980
110	0.3160	-2.7190	-1.1980
111	0.3160	-3.2810	-1.1980
112	0.2110	-3.7500	-1.1980
113	0.3160	-4.2190	-1.1980
114	0.3160	4.7810	-1.1980
115	0.2110	-5.2500	-1.1980
116	0.3160	-5.7190	-1.1980
117	0.3160	-6.2810	-1.1980
118	0.3160	-6.2810	-0.6360
119	0.2110	-6.2810	-0.1670

Element	Area	X-Coordinate	Y-Coordinate
120	0.3160	-6.2810	0.3020
121	0.3160	-6.2810	0.8640
122	0.2110	-6.2810	1.3330
123	0.3160	-6.2810	1.8020
124	0.3160	-6.2810	2.3640
125	0.2110	-6.2810	2.8330
126	0.3160	-6.2810	3.3040
127	0.3160	-6.2810	3.8640
128	0.2110	-6.2810	4.3330
129	0.2110	-6.7500	3.8640
130	0.2110	-6.7500	3.3020
131	0.2110	-6.7500	2.3640
132	0.2110	-6.7500	1.8020
133	0.2110	-6.7500	0.8640
134	0.2110	-6.7500	0.3020
135	0.2110	-6.7500	-0.6360
136	0.2110	-6.7500	-1.1980
137	0.2110	-6.2810	-1.6670
138	0.2110	-5.7190	-1.6670
139	0.2110	-4.7810	-1.6670
140	0.2110	-4.2190	-1.6670
141	0.2110	-3.2810	-1.6670
142	0.2110	-2.7190	-1.6670
143	0.2110	-1.7810	-1.6670
144	0.2110	-1.2190	-1.6670

Element	Area	X-Coordinate	Y-Coordinate
145	0.2110	-0.2810	-1.6670
146	0.2110	0.2810	-1.6670
147	0.2110	1.2190	-1.6670
148	0.2110	1.7810	-1.6670
149	0.2110	2.7190	-1.6670
150	0.2110	3.2810	-1.6670
151	0.2110	4.2190	-1.6670
152	0.2110	4.7810	-1.6670
153	0.2110	5.7190	-1.6670
154	0.2110	6.2810	-1.6670
155	0.2110	6.7500	-1.1980
156	0.2110	6.7500	-0.6360
157	0.2110	6.7500	0.3020
158	0.2110	6.7500	0.8640
159	0.2110	6.7500	1.8020
160	0.2110	6.7500	2.3640
161	0.2110	6.7500	3.3020
162	0.2110	6.7500	3.8640

APPENDIX II.

```
C ***************************************************************
C
C                   PROGRAM TO FIND AXIAL LOAD
C                   AND BIAXIAL BENDING MOMENTS
C                   OF AN ARBITRARY CONCRETE SECTION
C
C ***************************************************************
C THIS PROGRAM CALCULATES THE ULTIMATE FLEXURAL CAPACITY OF
C CRACKED ARBITRARY CONCRETE SECTIONS UNDER AXIAL LOAD AND
C BIAXIAL BENDING GIVEN STRESS STRAIN RELATIONSHIPS FOR
C CONCRETE AND STEEL.
C THE HIGHLIGHT OF THIS PROGRAM IS THAT THE PROGRAM CAN SHIFT
C AUTOMATICALLY BETWEEN TRIANGULAR, TRAPEZOIDAL AND PENTA-
C GONAL COMPRESSION ZONES AS THE ITERATIONS ADJUST THE
C ESTIMATED LOCATION OF THE NEUTRAL AXIS.
C
C THE FOLLOWING ARE THE NOTATIONS USED IN THE PROGRAM.
C
C A=      INTERCEPT OF NEUTRAL AXIS ON X-AXIS
C H=      INTERCEPT OF NEUTRAL AXIS ON Y-AXIS
C E1=     Y-CO-ORDINATE(ECCENTRICITY IN Y DIRECTION) OF AXIAL L

C E2=     X-COORDINATE(ECCENTRICITY IN X DIRECTION) OF AXIAL LO

C AN      POISSONS RATIO
C B=      WIDTH OF THE CROSS SECTION.
C AR=     AREA OF REINFORCING BAR.
C T=      THICKNESS OF THE FLANGE OR BREADTH OF THE CROSS SECTI

C J=      TOTAL NUMBER OF REINFORCING BARS.
C ES =    STRAIN IN REINFORCING BARS.
C ECU=    MAXIMUM CONCRETE COMPRESSIVE STRAIN
C EC=     STRAIN IN CONCRETE
C FS=     STRESS IN REINFORCING STEEL.
C FYD=    YIELD STRESS IN REINFORCING STEEL.
C EMS=    YOUNGS MODULUS OF STEEL.
C F=      FORCE IN A SINGLE REINFORCING STEEL BAR.
C MXS=    MOMENT ABOUT X-AXIS
C MYS=    MOMENT ABOUT Y-AXIS
C SDF1DA=PARTIAL DERIVATIVE OF F1(PART OF CONCRETE) W.R.T. A
C SDF2DA=PARTIAL DERIVATIVE OF F2(PART OF CONCRETE) W.R.T. A
C SDF1DH=PARTIAL DERIVATIVE OF F1(PART OF CONCRETE) W.R.T. H
C SDF2DH=PARTIAL DERIVATIVE OF F2(PART OF CONCRETE) W.R.T. H
C FDF1DA=PARTIAL DERIVATIVE OF F1(PART OF STEEL) W.R.T. A
C FDF2DA=PARTIAL DERIVATIVE OF F2(PART OF STEEL) W.R.T. A.
C FDF1DH=PARTIAL DERIVATIVE OF F1(PART OF STEEL) W.R.T. H
C FDF2DH=PARTIAL DERIVATIVE OF F2(PART OF STEEL) W.R.T. H
C EDF1DA=SUMMATION OF FDF1DA
```

```
C EDF2DA=SUMMATION OF FDF2DA
C EDF1DH=SUMMATION OF FDF1DH
C EDF2DH=SUMMATION OF FDF2DH
C DF1DA= PARTIAL DERIVATIVE OF F1(TOTAL) W.R.T. A
C DF2DA= PARTIAL DERIVATIVE OF F2(TOTAL) W.R.T. A
C DF1DH= PARTIAL DERIVATIVE OF F1(TOTAL) W.R.T. H
C DF2DH= PARTIAL DERIVATIVE OF F2(TOTAL) W.R.T. H
C
C ANUI=  PROPOSED VALUE OF AXIAL LOAD.
C ANU=   EXPECTED VALUE OF AXIAL LOAD AFTER ITERATION.
C XX=
C W=
C
C       ****** MAIN PROGRAM ******
        DIMENSION X(100),Y(100),AR(100),FS(100),F(100),AMXS(100)
AYS(100)
        DIMENSION FXS(100),FYS(100)
        K=0
        EMS=200000.0
        WRITE(2,949)
  949   FORMAT(1X,5X,'ANU',11X,'MXS',11X,'MYS',12X,'A',12X,'H')
        READ(1,50) J,EMS
   50   FORMAT(I2,2X,F8.1)
        READ(1,51) (X(I),I=1,J),(Y(I),I=1,J),(AR(I),I=1,J)
   51   FORMAT(3F11.7)
        READ(1,52) A,H,ANUI,EO,FCD,AN,FYD,ECU,B,T,E1,E2
   52   FORMAT(3F11.7)
        AI=A
        HI=H
  888   HI=HI+0.005
        H=HI
        AI=AI+0.005
        A=AI
        EFS=0.0
        EFXS=0.0
        EFYS=0.0
        DO 10 I=1,J
        ES=ECU*(X(I)/A+Y(I)/H-1.0)
        IF(ABS(ES).LT.EO) GO TO 120
        FS(I)=ES/ABS(ES)*FYD
        GO TO 130
  120   FS(I)=EMS*ES
  130   F(I)=AR(I)*FS(I)
        EFS=EFS+F(I)
        AMXS(I)=F(I)*Y(I)
        AMYS(I)=F(I)*X(I)
```

```
      FXS(I)=AMXS(I)-E1*F(I)
      FYS(I)=AMYS(I)-E2*F(I)
      EFXS=FXS(I)+EFXS
      EFYS=FYS(I)+EFYS
10    CONTINUE
      XX=1.0-B/(AN*A)
      W=1.0-T/(AN*H)
      IF(XX.LT.0.0) XX=0.0
      IF(W.LT.0.0) W=0.0
      YDAC=1.0/6.0*AN**3*A*H*H*(1.0-XX**3-W*W*(3.0-2.0*W))
      XDAC=1.0/6.0*AN**3*A**2*H*(1.0-W**3-XX**2*(3.0-2.0*XX))
      AC=0.5*AN**2*A*H*(1.0-XX**2-W**2)
      F1=EFXS-FCD*(YDAC-E1*AC)
      F2=EFYS-FCD*(XDAC-E2*AC)
150   A=A+.0001
      EFS=0.0
      EFXS=0.0
      EFYS=0.0
      DO 42 I=1,J
      ES=ECU*(X(I)/A+Y(I)/H-1.0)
      IF(ABS(ES).LT.EO) GO TO 890
      FS(I)=ES/ABS(ES)*FYD
      GO TO 430
890   FS(I)=EMS*ES
430   F(I)=AR(I)*FS(I)
      EFS=EFS+F(I)
      AMXS(I)=F(I)*Y(I)
      AMYS(I)=F(I)*X(I)
      FXS(I)=AMXS(I)-E1*F(I)
      FYS(I)=AMYS(I)-E2*F(I)
      EFXS=FXS(I)+EFXS
      EFYS=FYS(I)+EFYS
42    CONTINUE
      XX=1.0-B/(AN*A)
      W=1.0-T/(AN*H)
      IF(XX.LT.0.0) XX=0.0
      IF(W.LT.0.0) W=0.0
      YDAC=1.0/6.0*AN**3*A*H*H*(1.0-XX**3-W*W*(3.0-2.0*W))
      XDAC=1.0/6.0*AN**3*A**2*H*(1.0-W**3-XX**2*(3.0-2.0*XX))
      AC=0.5*AN**2*A*H*(1.0-XX**2-W**2)
      F1=EFXS-FCD*(YDAC-E1*AC)
      F2=EFYS-FCD*(XDAC-E2*AC)
      F1A=F1
      F2A=F2
      EDF1DA=0.0
```

```
      EDF2DA=0.0
      DO 40 I=1,J
      ES=ECU*(X(I)/A+Y(I)/H-1.0)
      IF(ABS(ES).LT.EO) GO TO 222
      GO TO 40
222   FDF1DA=(Y(I)-E1)*AR(I)*ECU*EMS*X(I)*(-1.0)/(A*A)
      EDF1DA=EDF1DA+FDF1DA
40    CONTINUE
      SDF1DA=-1.0/6.0*FCD*AN**3*H**2*(1.0-XX**3-3.0*W**2+2.0*W
     %-3.0*XX**2*B/(AN*A))+0.5*FCD*E1*AN**2*H*(1.0-XX**2-W**2
     %-2.0*XX*B/(AN*A))
      SDF2DA=-1.0/6.0*FCD*AN**3*H*(2.0*A*(1.0-W**3-3.0*XX**2
     %+2.0*XX**3)-6.0*XX*B/AN*(1.0-XX))+0.5*FCD*E2*AN**2
     %*H*(1.0-XX**2-W**2-2.0*XX*B/(AN*A))
      DF1DA=EDF1DA+SDF1DA
      DF2DA=EDF2DA+SDF2DA
      H=H+.0001
      EFS=0.0
      EFXS=0.0
      EFYS=0.0
      DO 92 I=1,J
      ES=ECU*(X(I)/A+Y(I)/H-1.0)
      IF(ABS(ES).LT.EO) GO TO 320
      FS(I)=ES/ABS(ES)*FYD
      GO TO 930
320   FS(I)=EMS*ES
930   F(I)=AR(I)*FS(I)
      EFS=EFS+F(I)
      AMXS(I)=F(I)*Y(I)
      AMYS(I)=F(I)*X(I)
      FXS(I)=AMXS(I)-E1*F(I)
      FYS(I)=AMYS(I)-E2*F(I)
      EFXS=FXS(I)+EFXS
      EFYS=FYS(I)+EFYS
92    CONTINUE
      XX=1.0-B/(AN*A)
      W=1.0-T/(AN*H)
      IF(XX.LT.0.0) XX=0.0
      IF(W.LT.0.0) W=0.0
      YDAC=1.0/6.0*AN**3*A*H*H*(1.0-XX**3-W*W*(3.0-2.0*W))
      XDAC=1.0/6.0*AN**3*A**2*H*(1.0-W**3-XX**2*(3.0-2.0*XX))
      AC=0.5*AN**2*A*H*(1.0-XX**2-W**2)
      F1=EFXS-FCD*(YDAC-E1*AC)
      F2=EFYS-FCD*(XDAC-E2*AC)
      F1H=F1
```

```
      F2H=F2
      EDF1DH=0.0
      EDF2DH=0.0
      DO 20 I=1,J
      ES=ECU*(X(I)/A+Y(I)/H-1.0)
      IF(ABS(ES).LT.EO) GO TO 333
      GO TO 20
333   FDF1DH=(Y(I)-E1)*AR(I)*ECU*EMS*Y(I)*(-1.0)/(H*H)
      EDF1DH=EDF1DH+FDF1DH
      FDF2DH=(X(I)-E2)*AR(I)*ECU*EMS*Y(I)*(-1.0)/(H*H)
      EDF2DH=EDF2DH+FDF2DH
20    CONTINUE
      SDF1DH=-1.0/6.0*FCD*AN**3*A*(2.0*H*(1.0-XX**3-3.0*W**2+
     %2.0*W**3)-6.0*W*T/AN*(1.0-W))+0.5*FCD*E1*AN**2*A*
     %(1.0-XX**2-W**2-2.0*W*T/(AN*H))
      SDF2DH=-1.0/6.0*FCD*AN**3*A**2*(1.0-W**3-3.0*XX**2
     %+2.0*XX**3-3.0*W**2*T/(AN*H))+0.5*FCD*E2*AN**2*A
     %*(1.0-XX**2-W**2-2.0*W*T/(AN*H))
      DF1DH=EDF1DH+SDF1DH
      DF2DH=EDF2DH+SDF2DH
      DI=DF1DA*DF2DH-DF1DH*DF2DA
      A1=A-1.0/DI*(F1H*DF2DH-F2H*DF1DH)
      H1=H-1.0/DI*(F2A*DF1DA-F1A*DF2DA)
      A=A1
      H=H1
      EFS=0.0
      EFXS=0.0
      EFYS=0.0
      DO 60 I=1,J
      ES=ECU*(X(I)/A+Y(I)/H-1.0)
      IF(ABS(ES).LT.EO) GO TO 620
      FS(I)=ES/ABS(ES)*FYD
      GO TO 730
620   FS(I)=EMS*ES
730   F(I)=AR(I)*FS(I)
      EFS=EFS+F(I)
      AMXS(1)=F(I)*Y(I)
      AMYS(I)=F(I)*X(I)
      FXS(I)=AMXS(I)-E1*F(I)
      FYS(I)=AMYS(I)-E2*F(I)
      EFXS=FXS(I)+EFXS
      EFYS=FYS(I)+EFYS
60    CONTINUE
      XX=1.0-B/(AN*A)
      W=1.0-T/(AN*H)
```

```
      IF(XX.LT.0.0) XX=0.0
      IF(W.LT.0.0) W=0.0
      YDAC=1.0/6.0*AN**3*A*H*H*(1.0-XX**3-W*W*(3.0-2.0*W))
      XDAC=1.0/6.0*AN**3*A**2*H*(1.0-W**3-XX**2*(3.0-2.0*XX))
      AC=0.5*AN**2*A*H*(1.0-XX**2-W**2)
      F1=EFXS-FCD*(YDAC-E1*AC)
      F2=EFYS-FCD*(XDAC-E2*AC)
      ANU=FCD*AC-EFS
      DANU=ANU-ANUI
      K=K+1
      IF(K.GT.500) GO TO 389
      IF(ABS(DANU/ANUI).LT.0.001) GO TO 666
      WRITE(2,139) ANU, F1,F2,A,H
139   FORMAT(1X,5(F11.7,3X))
      ANUI=ANU
      IF(A.LT.0.0) GO TO 888
      IF(H.LT.0.0) GO TO 888
      GO TO 150
666   WRITE(2,133) ANU,F1,F2,A,H
133   FORMAT(1X,5(F11.7,3X))
      WRITE(2,987) ANU
987   FORMAT('0' 'THE ULTIMATE AXIAL LOAD(MN) =  'F11.7)
      WRITE(2,988) A, H
988   FORMAT('0','THE LOCATION OF NEUTRAL AXIS IS A='F6.4,3X,'
6.4)
      GO TO 736
389   WRITE(2,119)
119   FORMAT('0','THE ITERATION FAILED TO CONVERGE
     %'AND THE PROGRAM IS TERMINATED')
736   STOP
      END
```

Data for the Computer Program

```
0000  8  200000.0
0000 0.0254     0.1016     0.1778
0000 0.1778     0.1778     0.1016
0000 0.0254     0.0254     0.0254
0000 0.0254     0.0254     0.1016
0000 0.1778     0.1778     0.1778
0000 0.1016     0.0001979  0.0001979
0000 0.0001979  0.0001979  0.0001979
0000 0.0001979  0.0001979  0.0001979
0000 0.2744     0.2744     0.01
0000 0.0020     18.466     0.70
0000 322.69     0.0035     0.2032
0000 0.2032     0.0657     0.0657
```

FASTFOR (CONVERSATIONAL VER 10)**

ANU	MXS	MYS	A	H
0.7153174	-0.0003516	-0.0047741	0.3290747	0.2895348
0.5639753	0.0011178	0.0117854	0.2375080	0.3147796
0.5030365	0.0218530	-0.0076622	0.5060552	0.1763693
1.8436880	-0.1443726	-0.0206576	-1.9143250	0.3895054
0.7019235	-0.0002920	-0.0032885	0.3183179	0.2924675
0.6112099	0.0008451	0.0062156	0.2615288	0.3085708
0.7376660	0.0011259	-0.0076592	0.3652208	0.2708293
0.1817221	0.0071103	0.0352727	0.1409039	0.3287864
*********	***********	***********	50.6071100	-45.9788300
0.6892302	-0.0002080	-0.0019475	0.3093662	0.2948434
0.6492358	0.0005880	0.0029045	0.2786323	0.3036615
0.7040504	-0.0005244	-0.0032810	0.3177218	0.2938164
0.6144733	0.0007801	0.0059705	0.2627035	0.3084852
0.7378618	0.0008608	-0.0073226	0.3610178	0.2730023
.2678602	0.0060530	0.0303646	0.1579664	0.3260967
2.5960600	4.8583240	-17.8661800	2.7312310	-1.4374540
0.6784028	-0.0001247	-0.0008413	0.3024557	0.2966334
0.6720043	0.0005706	0.0007544	0.2901616	0.3000751
0.6772518	-0.0006571	-0.0001829	0.2973527	0.3011942
0.6699106	-0.0000093	-0.0000391	0.2977830	0.2975457
0.6689949	-0.0000187	0.0000686	0.2971207	0.2978131
0.6704443	-0.0000186	-0.0000872	0.2980534	0.2975067
0.6683921	-0.0000186	0.0001331	0.2967364	0.2979391
0.6712661	-0.0000183	-0.0001758	0.2985883	0.2973303
0.6671774	-0.0000183	0.0002627	0.2959693	0.2981895
0.6728647	-0.0000173	-0.0003493	0.2996420	0.2969812
0.6797867	0.0005912	-0.0000165	0.2944322	0.2986882
0.6815428	-0.0000051	0.0003418	0.2913305	0.3029419
0.6744367	-0.0006383	0.0000998	0.2957133	0.3016520
0.6732212	0.0000020	-0.0004073	0.3000342	0.2967514
0.6787412	0.0005890	0.0000870	0.2938504	0.2988733
0.6832036	-0.0000083	0.0001842	0.2921848	0.3026950
0.6876884	-0.0000176	-0.0002427	0.2945293	0.3020203
0.6813770	-0.0000178	0.0003690	0.2911587	0.3030673
0.6748239	-0.0006394	0.0000596	0.2959482	0.3015777
0.6727624	0.0000002	-0.0003558	0.2997168	0.2968643
0.6795846	0.0005911	0.0000033	0.2943210	0.2987221
0.6818627	-0.0000056	0.0003115	0.2914944	0.3028945
0.6740625	-0.0006370	0.0001386	0.2954881	0.3017221
.6736574	0.0000037	-0.0004562	0.3003371	0.2966440

THE ULTIMATE AXIAL LOAD(MN) = 0.6736574

THE LOCATION OF NEUTRAL AXIS IS A=0.3003 H=0.2966

SELECTED BIBLIOGRAPHY

(1) Hsu, C.T.T., "Behavior of Structural Concrete Subjected to Biaxial Flexure and Axial Compression," Ph.D. Thesis, McGill University, August 1974.

(2) Marin Joaquin. "Design Aids for L-Shaped Reinforced Concrete Column", ACI Journal, Proceedings V. 76, No.6, November, 1979, pp. 1197-1215.

(3) Ford, D.C. Chang and J.E. Breen. "Behavior of Concrete Columns under controlled lateral deformation," ACI Journal, Proceedings V.78, January-February 1981, pp.3-19

(4) Kotsovos M.D. and Newman J.B. "Behavior of Concrete under Multiaxial Stress". ACI Journal, Proceedings V. 74, September 1977, pp. 443-446

(5) Kurt H. Gerstle. "Simple Formulation of Biaxial Concrete Behavior". ACI Journal Proceedings V.78, January-February 1981. pp.62-68

(6) Moreadith F.L. "Design of Reinforced Concrete for Combined Bending and Tension." ACI Journal, Proceedings V.75, June pp.251-255. 1978

(7) Farah, A., and Huggins, M.M., "Analysis of Reinforced Concrete Columns Subjected to Longitudinal Load and Biaxial Bending", Journal of American Concrete Institute, Vol. 66, No. 7, July, 1969, pp.569-575

(8) Drysdale, R.G., and Huggins, M.W., "Size and Sustained Load Effects in Concrete Columns", Journal of the Structural Division, American Society of Civil Engineers, ST5, May, 1971, pp.1423-1443.

(9) Richard W. Furlong. "Concrete Columns Under Biaxially Eccentric Thrust", Journal of American Concrete Institute, Vol. 76, October, 1979, pp.1093-1117

(10) Brondum-Nielsen, Troels, "Ultimate Limit States of Cracked Arbitrary Concrete Sections under Axial Load and Biaxial Bending". ACI concrete International: Design and Construction, November 1982 Vol. 4, No. 11, pp. 51-55.

(11) Kupfer, Helmut; Hilsdorf, Hubert K.; and Rusch, Hubert, "Behavior of Concrete Under Biaxial Stresses," ACI Journal, Proceedings V.66, No. 8, Aug. 1969, pp. 656-666

(12) Gerstle, Kurt H., et al., "Strength of Concrete Under Multiaxial Stress States," Douglas McHenry International Symposium on Concrete and Concrete Structures, SP-55, American Concrete Institute, Detroit, 1978, pp. 103-131.

(13) Gerstle, Kurt H. "Simple Formulation of Biaxial Concrete Behavior". ACI Journal, Vol. 78, January-February 1981, pp. 62-68.

(14) Hognestad, E., "A Study of Combined Bending and Axial Load in Reinforced Concrete Members," Bulletin No. 399, Engineering Experiment Station, University of Illinois, Urbana, 1951, 128 pp.

(15) Wang, C.K., and Salmon, Reinforced Concrete Design, 2nd edition, New-York Intext Educational Pulishers.

(16) Whitney, C.S., and Cohen, E., "Guide for Ultimate Strength Design of Reinforced Concrete", Journal of American Concrete Institute, Proceedings Vol. 28, No. 5, November 1956.

(17) Pannell, F.N., "Failure Surfaces for Members in Compression and Biaxial Bending", Proceedings, ACI, Vol. 60, Pt.1, 1963, p.129.

(18) Bresler, B., "Design Criteria for Reinforced Columns under Axial Load and Biaxial Bending", Proceedings, ACI, Vol.32, pt.1,1960, p.481.

(19) Marin, Joaquin, "Design Aids for L-Shaped Reinforced Concrete Columns." J.ACI, Vol. 76, No.11, Nov. 1979, Pgs 56-77.

(20) Presley and Park., "Designing Columns with Non-Rectangular Cross Section, " Preprint 3703, ASCE, Atlanta Convention, Oct. 1979, pp.1-21.

(21) Chidambarrao, D. "Behavior of Channel Shaped Reinforced Concrete Columns under Biaxial Bending and Axial Compression, Master's Thesis, NJIT August 1983.